The potential of hyperspectral remote sensing in determining water turbidity as a water quality indicator

Dumisani Solly Mashele

203513086

A thesis submitted to the School of Agricultural, Earth and Environmental Sciences, at the University of KwaZulu-Natal, in partial fulfillment of the academic requirements for the degree of Master of Environment and Development (MEnvDev), Land Information Management

March 2013

Pietermaritzburg

South Africa

DECLARATION

This research work was undertaken in partial fulfillment of a Master of Environment and Development (MEnvDev), Land Information Management offered through the School of Agricultural, Earth and Environmental Sciences. I would like to declare that the research work reported in this thesis has never been submitted in any form for any degree or diploma to any tertiary institution. It, therefore, represents my original work .Where use has been made of the work of other authors or organizations it is duly acknowledged within the text and references list.

Dumisani Solly Mashele
(203513086)

Signed: ___________________________________Date:_________________

As the candidate's supervisor, I certify the above statement and have approved this thesis for submission.

Dr John Odhiambo Odindi

Signed: ___________________________________Date:_________________

PLAGIARISM DECLARATION

I, Dumisani Solly Mashele, declare that:

1. The research reported in this thesis, except where otherwise indicated is my original work.
2. This dissertation has not been submitted for any degree or examination at any other university.
3. This dissertation does not contain other persons' data, pictures, graphs, or other information, unless specifically acknowledged as being sourced from other persons.
4. This dissertation does not contain other persons' writing, unless specifically acknowledged as being sourced from other researchers. Where other written sources have been quoted, then:
   a. Their words have been re-written, but the general information attributed to them has been referenced.
   b. Where their exact words have been used, then their writing has been placed in italics and inside quotation marks, and referenced.
5. This dissertation does not contain text, graphics, or tables copied and pasted from the Internet, unless specifically acknowledged and the source being detailed in the thesis and in the References Section.

Signed: ________________________________

TABLE OF CONTENTS

LIST OF FIGURES

LIST OF TABLES

ABSTRACT

Globally, water turbidity remains a crucial parameter in determining water quality. South Africa is largely regarded as arid and is often characterised by limited but high intensity rainfall. This characteristic renders most of the country's water bodies turbid. Consequently, the use of turbidity as a measure of water quality is of great relevance in a South African context. Generally, turbidity alters biological and ecological characteristics of water bodies by inducing changes in among others temperature, oxygen levels and light penetration. These changes may affect aquatic life, ecosystem functioning and available water for industrial and domestic use. Siltation, a direct function of turbidity also impacts on the physical storage of dams and shortens their useful life. To date, determination of water turbidity relies on the tradition laboratory based methods that are often time consuming, expensive and labour intensive. This has increased the need for more cost effective means of determining water turbidity.

In the recent past, the use of remote sensing techniques has emerged as a viable option in water quality assessment. Hyperspectral remote sensing characterizes numerous contiguous narrow bands that have great potential in water turbidity measurement. This study explored the applicability of hyperspectral data in water turbidity detection. It explored the visible and near-infrared region to select the optimal bands and indices for turbidity measurement. Using the Analytical Spectral Device (ASD) field spectroradiometer and a 2100Q portable turbidimeter, spectral reflectance and laboratory based turbidity measurements were taken from prepared turbid solutions of predetermined concentrations (i.e. 10g/l to 150g/l), respectively. The Pearson's coefficient of correlation and R^2 values were employed to select optimal spectral bands and indices. The findings showed a positive linear relationship between reflectance, the amount of soil in water and turbidity values. The strongest relationships came from bands 528, 489, 657, 1000 and 983, reporting adjusted R^2 values of 0.7062, 0.7004, 0.6864, 0.7120 and 0.6961, respectively. The highest coefficient came from band 1000nm. The strongest indices were 625/440 and (770-1000)/(770+1000), with adjusted R^2 values of 0.6822 and 0.6973 respectively. The use of hyperspectral data in turbidity detection is ideal for optimal band interrogation. Although good results were generated from this study, further investigations are needed in the near-infrared region.

ACKNOWLEDGEMENTS

Firstly, I wish to express my deepest gratitude to the Almighty God for the grace He has extended to me by His son and my Lord Jesus Christ. You are the sum total of all my endeavours.

My sincere appreciation goes to my supervisor Dr JO Odindi for his motivation, guidance, patience and support throughout the research. Without him this work would have not been successful.

I thank Dr E Adam for his excellent assistance and advices on data collection, preparation and analysis. My knowledge and technical skills in remote sensing have improved immensely because of you.

To my colleague and brother, Mr C Adjorlolo, thank you for the ideas, academic interrogations and honest feedback to my seemingly never-ending questions. You helped sharpen my understanding in research.

I extend my gratitude to my boss Mrs. FJ Mitchell for her continued understanding and support and also to the Department of Agriculture and Environmental Affairs for helping with the soil and water analyses.

To my parents (Mr PJ and Mrs. M Mashele), brothers (Sifiso and Luyanda) and sisters (Olgar, Siphiwe and Thobile), thank you for always believing in me. Your love and support have continued to propel me forward to succeed.

Finally, I want to thank my beautiful wife, Portia Nombuso Ngcobo (now a Mashele), for being a true friend, my personal chief advisor, my strength and number one supporter. I love you always.

CHAPTER 1: INTRODUCTION

1.1 Introduction

Water constitutes three quarters of the Earth's surface (Plaza et al., 2004). Of that amount only 2.5% is fresh-water and exists as permanent snow cover and glaciers, groundwater, soil, swamps, lakes and rivers (Shiklomanov, 1998). Due to a rise in population, industrial development and expansion of irrigation agriculture, water use has increased six-fold over a period of 70 years (Bernstein, Undated). The quality of available water has also declined. According to Bernstein (Undated), about 1.1 billion people are deprived of clean water. Poor water quality is reported as one of the leading causes of death in poor communities (Venter, 2002, WRC, 1998).

Over 65% of the African continent is classified as arid or semi-arid (Clark, 2010). Clark (2010) further notes that the continent accounts for only 9% of global renewable freshwater resources. Environmental related threats like forest and biodiversity loss, land degradation and urbanization caused by ever increasing population have further led to a decline in water quality and quantity (Clark, 2010, Eva et al., 2006). Like other African countries, South Africa is characterised by perennial water stress and scarcity (Eva et al., 2006).

With an average total annual rainfall of 450mm compared to the world's 860mm, South Africa is regarded as a semi-arid country (CSIR, 2010). Over 90% of her mean annual rainfall is lost to the atmosphere through evaporation (Whitmore, 1971 as cited by Schulze, 1995) and only about 8.5% of the available water translates to runoff (Backeberg et al., 1996). A large portion of the available water is often allocated for use, leaving virtually no surplus water. Furthermore, the country's fast growing population, changing standard of living and recent government drive to establish "decent" human settlements has further increased pressure on the existing water resources (Ashton, 2007, CSIR, 2010, Fatoki et al., 2001). Increased volumes for domestic, industrial and agricultural, mining and power generation have combined with land use associated problems like soil erosion to degrade the quality of the country's water resources (CSIR, 2010, Du Plessis, 2006).

1.1.1 *Turbidity and water quality*

Turbidity is an important water quality indicator that measures the relative clarity of water (Lambrou et al., 2010). It basically amounts from suspended silt and clay particles, algae, organic matter and microscopic organisms in water bodies affect their color and brightness (Kwoh et al., Undated, Ramollo, 2008). Generally, turbidity interferes with a water body's light transmission which affects submerged aquatic plant's primary productivity (Hart, 1999, Norsaliza and Hasmadi, 2010a, Norsaliza and Hasmadi, 2010b, Ramollo, 2008). Furthermore, turbidity reduces the amount of oxygen in water which may cause plant death, organic matter decay and induce production of carbonic acid (Hart, 1999). The subsequent suppressed production in aquatic plants reduces food availability, which in turn affects biota distribution and habitat selection (Dörgeloh, 1995, Hart, 1999). Because suspended particles absorb more sunlight they increase water temperature, leading to further depletion of dissolved oxygen as warm water holds less oxygen than cool water (Ramollo, 2008). These conditions lead to aesthetically undesirable and un-inhabitable water bodies devoid of life.

South Africa's water resources are particularly affected by turbidity. Almost all of the country's reservoirs are turbid (Dörgeloh, 1995, Dörgeloh et al., 1993). The country's reserviors turbidity levels are largely attributed to arid conditions associated with high intensity rainfalls on areas with limited vegetation and consequent soil erosion (Hart, 1999). Other turbidity causative factors include domestic and industrial effluents and agrochemicals from agriculture (Ashton, 2007). Ultimately most of the water from these sources is drained into rivers.

Turbidity does not only have environmental and ecological consequences in river systems but also pose an economic threat, through facilitating reservoir siltation. Such makes its measurement and monitoring a valuable exercise. Traditional methods used to determine turbidity like *in situ* measurements and laboratory analyses play a significant role in monitoring water quality. However, these techniques are time-consuming, expensive and labour intensive (He et al., 2008, Liu et al., 2003, Shafique et al., 2003, Su et al., 2008b, Yang et al., 2000, Yang and Jin, 2010). Generally, the use of these techniques is often required for wider temporal and spatial scale, which remains a challenge (Bierman et al., 2011).

Turbidity analysis using remote sensing techniques offers a great opportunity in water quality management. These techniques permit for more efficient data collection and analyses, which offer opportunities to identify other implicit relationships (Koponen, 2006, Senay et al., 2001). Recent improvement in sensor spatial and spectral resolutions and point based spectroscopy has facilitated the investigation of various aspects of water quality. A number of studies have successfully explored remote sensing application techniques in water quality. These studies have investigated the water quality parameters that include among others pH, salinity, chlorophyll *a*, total phosphorus and temperature, total suspended sediments and turbidity (Akbar et al., Undated, He et al., 2008, Norsaliza and Hasmadi, 2010a, Norsaliza and Hasmadi, 2010b, Pavelsky and Smith, 2009, Su et al., 2008a, Wu et al., 2007, Zhengjun et al., 2008). What is limiting about most of these studies is that they used broad band spectral categorization of reflected and emitted energy, covering the visible to near-infrared regions (Govender et al., 2007). The use of hyperspectral remote sensing using a spectrometer permits several hundreds of spectral bands to be collected at one time. This characteristic offers the opportunity to explore and discover algorithms appropriate for the accurate estimation of water quality parameters such as turbidity (Govender et al., 2008).

1.2 Aim of the study

This study aims at exploring the potential utility of spectral reflectance in characterizing turbidity. The study combines conventional laboratory soil turbidity measurements with spectral reflectance measurements from turbid solutions to identify correlations and select the optimal bands for turbidity estimations.

1.3 Research objectives

This study is based on the following objectives:

1. Investigating the relationship between turbidity levels and spectral reflectance.
2. Identifying and select optimal spectral bands that can potentially be used to estimate turbidity levels.

The objectives of this study will be achieved by collecting soil samples which will be analysed for mineralogy and other physio-chemical measures. This will be trailed by an experimental design where a series of water samples with varying amounts of soil in a known volume of water will be determined for turbidity levels in the laboratory. Concurrently, the spectral reflectance of each sample will be measured.

1.4 Structure of thesis

Chapter 1

The first chapter gives a general introduction, background, problem statement, the study's objectives and structure of the thesis.

Chapter 2

This chapter will deal with a review of literature and previous developments in water quality monitoring. A comprehensive review of the world's water resources and water quality challenges will be presented. Thereafter, the severity and impact of poor quality in the context of South Africa will be dealt with, highlighting the sources and nature of pollution in question. The scope on turbidity, its causes and holistic effects on the water resources will then be presented. The chapter will conclude by discussing the use of remote sensing in the estimation of water quality parameters, particularly turbidity.

Chapter 3

In the methodology chapter, the data, apparatus and techniques employed are discussed. The chapter focuses on data collection methods, assumptions, norms and accuracy.

Chapter 4

This chapter presents and describes the results obtained from the soil analysis, spectral and laboratory measured turbidity. It presents and describes the spectral variables (i.e. bands and indices) that display a strong relationship with turbidity.

Chapter 5

This chapter is dedicated to a thorough discussion of the implications of the results. Each spectral band is examined according to its relevance in turbidity detection. This is followed by conclusions on the applicability of hyperspectral data in turbidity detection, the optimal spectral bands and recommendations on the direction for further research.

CHAPTER 2: LITERATURE REVIEW

2.1 Water resources

2.1.1 Water resources: a general outlook

Water is a critical source of life. Water covers three quarters of the Earth's surface and is held in oceans and freshwater bodies (Norsaliza and Hasmadi, 2010b, Plaza et al., 2004). Both water bodies play vital roles in biotic and abiotic systems. Of all the global water, freshwater constitutes only 2.5%, of which 68.9% is trapped in glaciers and permanent snow, 29.9% is stored underground, and 0.9% exists as soil moisture, swamp water and permafrost. Of the total amount of water on the Earth's surface, only 0.3% is found in rivers and lakes (Shiklomanov, 1998). It is this meagre 0.3% that is available for domestic, agricultural, industrial and recreational use (Razmkhah et al., 2010).

With over 65% of the surface area classified as arid or semi-arid, Africa faces the greatest water related challenges as she accounts for only 9% of global renewable freshwater resources (Clark, 2010). Moreover, Africa's growing population, with the highest birth–rate, is reported to have exceeded the capacity of natural resources to meet her population's needs in many areas. This has led to among others loss of forests and biodiversity, land degradation, and declining quality and quantity of water (Clark, 2010, Eva et al., 2006). According to Eva et al., (2006), water stress and scarcity are now attributed as endemic in almost a quarter of all African countries including South Africa.

2.1.2 Water resources in South Africa

With an average annual rainfall of 450mm compared to the global 860mm per annum, South Africa is regarded as a dry country (CSIR, 2010). Furthermore, the existing rainfall is highly variable and poorly distributed across the country (CSIR, 2010, Earle et al., 2005). According to Whitmore, 1971 (as cited by Schulze, 1995), it is estimated that of the mean annual rainfall received in the country, over 90% is lost to the atmosphere through evaporation and only about 8.5% of the rainfall is translated to runoff and therefore available for use as lakes and rivers (Backeberg et al., 1996). With very limited permanent standing waters in the country, rivers are the source of almost all exploitable surface water (Day et al., 1986).

In addition to the high demand for ecosystem functioning, the country's fast growing population, changing standard of living and the recent government drive to provide settlements has further put a strain on the existing fresh water resources (Ashton, 2007, CSIR, 2010, Fatoki et al., 2001). Whereas a number of efforts like building of 500 dams and inter catchment water transfers have been initiated, such efforts have been seriously impaired by the deterioration of existing water quality (CSIR, 2010, Earle et al., 2005, NWRS, 2004).

2.2 Water quality

Poor water quality is regarded as one of the leading causes of death, particularly in poor communities (Venter, 2002). Poor quality water not only limits the water's utilization value but also increases among others treatment costs, waterborne disease outbreaks and decline in agro-based trade due to health concerns (Cairns et al., 1997, CSIR, 2010). Poor quality also reduces the resource's availability because the poorer the quality of water, the less likely will it be able to support various uses (Ngwenya, 2006).

The Department of Water Affairs (DWA), summarizes water quality as a function of its physical, chemical, biological and ecological attributes (Du Plessis, 2006, NWRS, 2004) while others like Du Plessis (2006) describe it as a synergy of the water's physical and chemical attributes that render it useful for a specific purpose. According to Venter (2002), dissolved and suspended substances affect the suitability of water for the variety of uses.

2.2.1 Physical attributes

The physical attributes of water encompass all features that can be measured using physical methods (Du Plessis, 2006, Venter, 2002). Examples to these attributes are pH, electrical conductivity, total dissolved solids, turbidity and temperature. Their effect is predominantly on the aesthetic as well as the chemical composition of the water.

2.2.2 Chemical attributes

These serve to describe the nature and concentrations of substances dissolved in water (Du Plessis, 2006). Such substances can be organic or inorganic compounds, metals, and other kinds of minerals. Although some of the substances dissolved in water can have a nutritional benefit to the biotic system, some are harmful particularly if they exist in higher levels and concentrations (Du Plessis, 2006). Chloride, sulphate, nitrate, nitrite, calcium, magnesium, manganese, aluminium and ammonium are some of the chemical constituents indicative of water quality.

2.2.3 Biological attributes

Biological attribute are the biological organisms found in a water body. Organisms are often indicative of the conditions in which they live (Day, 2000). Biological attributes have become a routine tool in the management of South Africa's inland water resources and plays a crucial role in the overall monitoring and assessment of water resources (de la Rey et al., 2004, Ramollo, 2008). Popular indicators include fish, algae and invertebrates (de la Rey et al., 2004).

2.3 Water quality in South Africa

2.3.1 A general overview

The threat and impact of declining water quality have not gone un-noticed in South Africa. Serious water quality concerns have been raised by both scientists and the public (Van der Merwe-Botha, 2009). Furthermore, decision makers, investors and researchers have highlighted possible negative impacts of poor water quality on the country's economy in both short and long term (Van der Merwe-Botha, 2009). Consequently, the DWA has recognised deteriorating water quality as "one of the major threats to South Africa's capability to provide sufficient water of appropriate quality to meet its needs and to ensure environmental sustainability" (NWRS, 2004: 22). However, relevant national water bodies have been monitoring water resources for planning, management and pollution control quality since late 1960s (Ngwenya, 2006, Van Vliet and Nell, 1986). According to the National Water Resource Strategy report of 2004, the DWA monitors the physio-chemical, microbial and biological water quality parameters of surface water together with eutrophication, toxicity and radioactivity (NWRS, 2004).

2.3.2 Causes of water pollution

Causes of the deteriorating water quality include among others domestic, industrial and agricultural wastes, irrigation return flows, fertilizers, pesticides, surface run-off, urban development, de-forestation, mining and power generation (CSIR, 2010, Du Plessis, 2006, NWRS, 2004). Because rivers act as natural drains on the surface, studies show that almost all South African rivers receive treated domestic and industrial effluent from urban areas, and return flows loaded with agrochemicals from agriculture (Ashton, 2007). Consequently, downstream dams are often polluted (CSIR, 2010). Other contributing factors include the country's outdated and inadequate water and sewage treatment infrastructure (CSIR, 2010). According to CSIR (2010), most of the country's urban sewage does not undergo proper treatment prior to discharge because of inadequacies in the sewer systems. Eroded soil and other material dislodged and transported by runoff into waterways cause salinity, eutrophication, disease-causing micro-organisms, turbidity, acidity and other forms of deteriorations (CSIR, 2010, Ngwenya, 2006).

2.4 Water turbidity

To monitor water quality specific parameters are quantified. Koponen (2006) lists parameters that are important in water quality monitoring as chlorophyll-*a*, suspended inorganic matter, coloured dissolved organic matter, turbidity, secchi depth and temperature among others. Turbidity is particularly important in South Africa because most of the reservoirs are regarded as turbid (Dörgeloh, 1995, Dörgeloh et al., 1993). The characteristic turbid conditions of the country's water bodies can be attributed to arid conditions associated with high intensity rainfalls favoring soil erosion (Hart, 1999). Contributions from domestic and industrial effluent discharged from urban areas, return flows from agricultural lands loaded with agrochemicals, logging, mining, road building as well as commercial construction are noted as the most common sources of water turbidity.

Commonly, turbidity is derived from suspended silt and clay particles, algae, air bubbles, organic matter together with microscopic organism in water bodies. These factors affect water color and brightness, giving it the typical murky colour (Han and Rundquist, 1998, Kwoh et al., Undated, Omar and MatJafri, 2009, Ramollo, 2008). Generally, turbidity is a measure of optical properties of water responsible for scattering and absorbing radiation (Norsaliza and Hasmadi, 2010a, Koponen, 2006, Kwoh et al., Undated, Han and Rundquist, 1998). It describes the reduction of transparency of a liquid following the presence of un-dissolved matter (Lambrou et al., 2010). Some authors refer to it as the measure of relative clarity of water (Lambrou et al., 2010, Norsaliza and Hasmadi, 2010b, Sadar, Undated). Turbidity measurement is critical in determining the impacts of agricultural, landscape and urban nutrient and sediment discharges and processes, predicting pollution loads and formulation of environmental and restoration management plans (Aghighi et al., 2008, Moreno-Madrinan et al., 2010)). Turbidity measurement is also a key indicator to the suitability of water for human consumption.

The impacts of turbidity are beyond the mere impediment to light transmission. It directly hampers photosynthesis thereby suppressing primary production and reducing oxygen levels (Norsaliza and Hasmadi, 2010a, Ramollo, 2008, Hart, 1999). Turbidity also suppresses production of food availability in aquatic ecosystems, which in turn affects biota distribution and habitat selection (Dörgeloh, 1995, Hart, 1999). Because suspended particles absorb more sunlight, water temperature is increased leading to further depletion of dissolved oxygen as warm water holds less oxygen than cool water (Ramollo, 2008). Turbidity also acts as an indicator to the presence of pathogens, providing them with food and shelter (Lambrou et al., 2010, Rizzo et al., 2005). This can promote pathogen re-growth consequently facilitating waterborne disease outbreaks (Rizzo et al., 2005, Lambrou et al., 2010). Turbidity can also lead to the loss of storage capacity of dams due to sedimentation, shortening their useful life (Bhatti et al., 2007). Consequently determination of water turbidity is critical for the management of water quality.

2.5 Turbidity measurement

One of the traditional techniques in turbidity measurement is the secchi disk. This is a circular plate painted black and white which is lowered into the water until it cannot be seen (Han and Rundquist, 1998, Jensen, 2000). The more turbid the water is the quicker it disappears from view. The drawback of this technique is its strong subjectivity to human visual perception (Jensen, 2000). The other technique of turbidity measurement involves a candle and flat-bottomed glass. This technique dates back to the 1900s, and is referred to as the Jackson Candle Turbidimeter (Sadar, Undated). The major limitation of this technique is its inability to measure very low turbid solutions caused by the use of longer wavelength light source (candle) and inferior detectors and optical geometry (Sadar, 2002, Sadar, Undated).

Two main categories of instruments are currently recognized in turbidity instruments; turbidimeters (or absorptiometers) and nephelometers (Lambrou et al., 2010, Minella et al., 2008, Omar and MatJafri, 2009). Turbidimeters measure the absorption of light intensity passing through a sample in relation to the initial beam (Omar and MatJafri, 2009, Lambrou et al., 2010, Minella et al., 2008). They are regarded to be the most appropriate for samples with particles larger than the wavelength of the light being used (Lambrou et al., 2010). Nephelometers, on the other hand, quantify the portion of light scattered from the incident beam within a wide angle centered at 90^o, reported in nephelometric units (NTUs) (Hongve and Åkesson, 1998, Lambrou et al., 2010, Omar and MatJafri, 2009, Peng et al., 2009, Sadar, Undated, Sadar and Engelhardt, Undated, Ziegler, 2002). Nephelometers are the most modern and internationally recognized instruments (Sadar, Undated, Ziegler, 2002, Sadar and Engelhardt, Undated, Omar and MatJafri, 2009), and are regarded as more precise and sensitive than turbidimeters, particularly when dealing with samples of low turbidity (Lambrou et al., 2010, Sadar, Undated).

Whereas the above mentioned methods have been critical in monitoring turbidity, they require intense calibration, elaborate sampling and subsequent laboratory analyses (Koponen, 2006, Akbar et al., Undated). They are also slow, time-consuming, expensive and labour intensive (Akbar et al., Undated, El-Masri and Rahman, Undated, He et al., 2008, Koponen, 2006, Sheela et al., 2010). Furthermore, these techniques do not provide near real-time results (Ramollo, 2008). However, recent remote sensing advancements offer a great opportunity for turbidity measurement and a basis for water quality management.

2.6 The application of remote sensing in water quality

Remote sensing is a process by which information about features on the Earth's surface is collected without the necessity of a physical contact between the instrument and the target (Koponen, 2006, Lillesand et al., 2004). Remote sensing instruments use sensors to record information about features. These sensors can be airborne (e.g aircrafts), spaceborne (satellites) or field-based. The instruments can also be either passive; that record solar radiation reflected by surface features to discern their properties, or active, that generate their own electromagnetic radiation (Koponen, 2006). In a remote sensing process, reflected, emitted or scattered electromagnetic radiation of a target is measured as a function of wavelength (Clark, 2010, Hellweger et al., 2004, Koponen, 2006).

Recording sensors are available as either panchromatic, multispectral or hyperspectral. Most multispectral sensors are characterized by three to six spectral bands, falling between the visible to near-infrared region of the electromagnetic spectrum (Govender et al., 2008). Hyperspectral sensors have a wider spectrum that extends from the visible, near-infrared, mid-infrared to shortwave infrared (Liu et al., 2009). Typically, hyperspectral remotely sensed data are characterized by huge amounts of data at a near-laboratory (high accuracy with little errors) quality in the contiguous narrow bands (Liu et al., 2009). This characteristic significantly extends the range to which remote sensing techniques can be applied (Liu et al., 2009). Field spectrometers, a type of hyperspectral instruments, have become popular means of collecting spectral data. They are very useful in establishing relationships between the spectral characteristics and biological, physical and chemical attributes of features (Novo et al., 2004). Generally, the successful application of remote sensing techniques lies in understanding how features interact with radiation energy (see Figure 1).

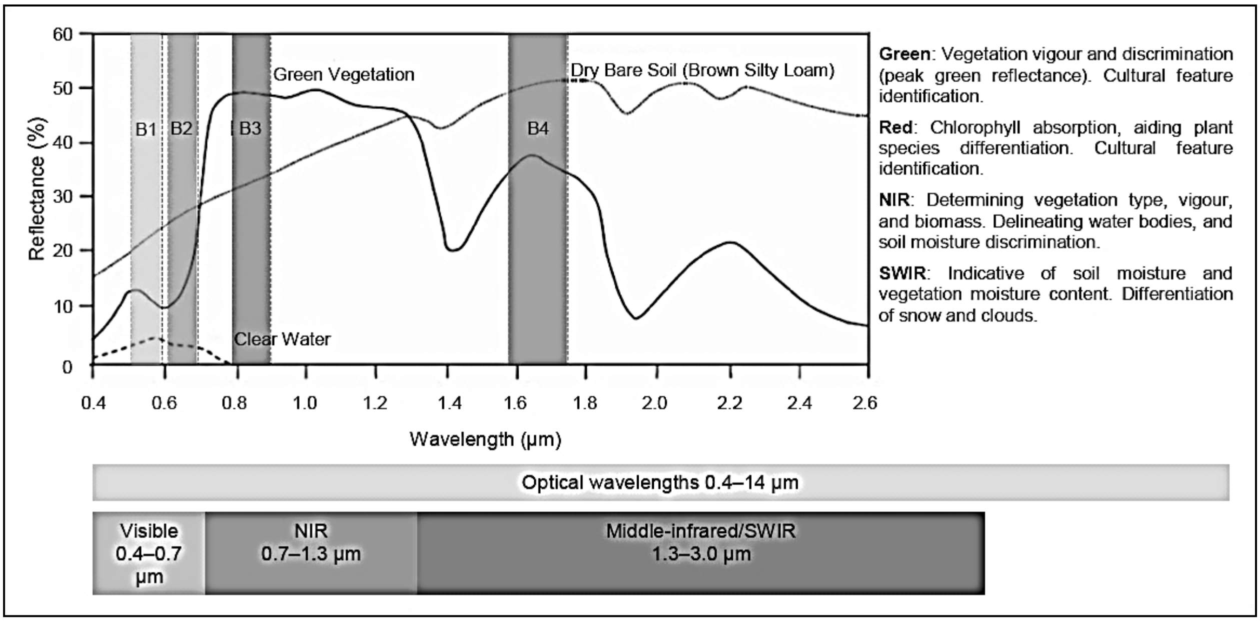

Figure 1: Spectral responses of common materials (Source: Clark, 2010)

Vegetation reflects at its minimum in the visible region, increasing sharply around 700nm (red edge) and highly in the near-infrared region. Soil and other bare surfaces comprise a steady increase across the visible and near-infrared spectrum (Clark, 2010). Clear water has a general spectral signature that peaks at around 400-500nm and exhibits total absorption in the near-infrared region. According to Jensen (2000) one of the distinct spectral responses of clear water is its absorption characteristic of almost all incident energy in the near-and middle-infrared (740-2500nm) portion of the spectrum. Most of the scattering occurs in the violet, dark blue and light blue categories (400-500nm) (Jensen, 2000). However, the presence of organic and inorganic constituents complicates the normal spectral response of water. In-water constituents favor near-infrared surface reflection and sub-surface volumetric scattering thereby causing significant scattering and reflection (Jensen, 2000). They also shift the reflectance peaks towards longer wavelengths (Chen et al., 1992, Doxaran et al., 2002). Such a characteristic is illustrated in Figure 2 below.

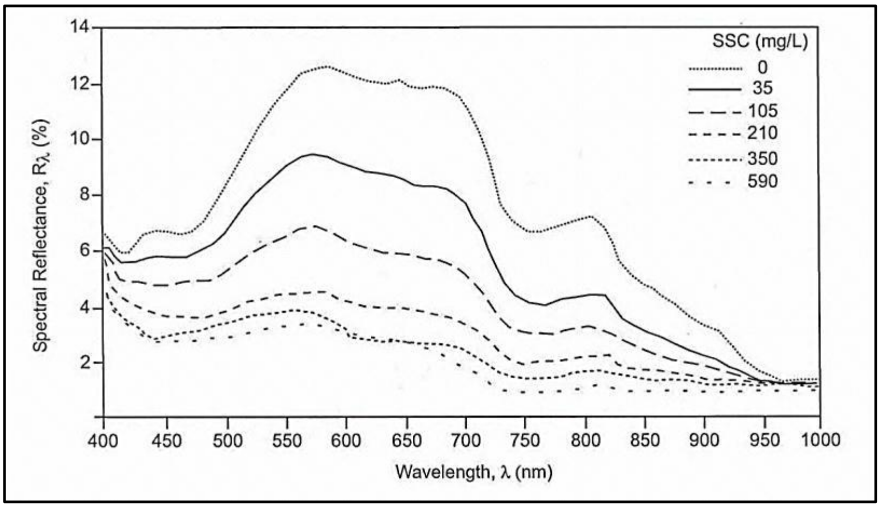

Figure 2: Change in reflectance against turbidity (After Chen et al., 1992)

The application of remote sensing in water resource management is not entirely new. In fact, aerial photographs, a form of remote sensing, have for decades been used to identify and examine water bodies (Krijgsman, 1994, Secor, 2006). Many studies have indicated that use of remote sensing techniques is more advantageous than traditional methods (He et al., 2008, Norsaliza and Hasmadi, 2010b). According to Zhengjun et al. (2008), remotely sensed datasets facilitate easier, rapid and seasonal water quality data collection at minimum costs. Other studies note that remote sensing methods permit for more focused and efficient field sampling, potentially reducing the number of samples required for a particular water body (Adam et al., 2010, Hellweger et al., 2004, Secor, 2006).

The above mentioned advantages, together with the availability of established techniques and improved precision in atmospheric and geometric corrections, makes it possible to employ remote sensing to accurately assess and monitor water quality constituencies (Turdukulov, 2003). Many algorithms for data interpretations and modeling have been developed (Santini et al., 2010). Numerous studies have used remote sensing to estimate a range of parameters such as pH, salinity, chlorophyll-*a*, total phosphorus, temperature and total suspended sediments (Chen, 2003, He et al., 2008, Norsaliza and Hasmadi, 2010a, Norsaliza and Hasmadi, 2010b, Pavelsky and Smith, 2009, Senay et al., 2001, Su et al., 2008b, Thiemann and Kaufmann, 2000, Volpe et al., 2011, Akbar et al., Undated, Wu et al., 2007). Whereas satisfactory relationships have been established for most marine water quality indicators, progress in inland freshwaters has been slow largely due to optical heterogeneity and turbid nature (Gons, 1999, Moore, 1980).

2.6.1 Estimating turbidity

Moore (1980) notes the possibility of quantifying turbidity from remotely sensed measurements and highlights the importance of considering the principles of light and water interaction. Such an interaction is described by four sources of electromagnetic energy (Figure 3).

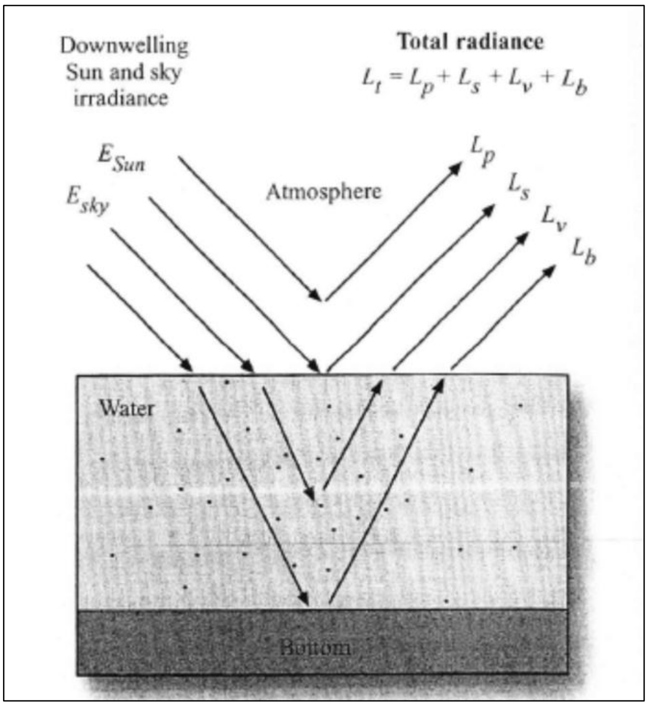

Figure 3: Sources of electromagnetic radiation (Source: Jensen, 2000)

As energy moves from the sun through the atmosphere, a portion of it is scattered and never reaches the water surface (L_p), while another portion manages to reach the air-water interface but barely penetrates the surface and is reflected away (L_s) (Jensen, 2000). This reflected energy may carry with it spurious surface reflectance due to wind-induced reflectivity and the presence of bubbles (Han and Rundquist, 1998). The portion that penetrates the water surface, reaches the bottom of the water body and then rises up to exit the water column, this constitutes the bottom radiance (L_b) (Jensen, 2000). According to Jensen (2000) and Liu et al. (2003) the later portion is useful for bathymetric or coral reef mapping. The portion that is crucial in water turbidity analyses is termed the subsurface volumetric radiance (L_v) (Koponen, 2006, Jensen, 2000). This portion manages to penetrate through the air-water interface, interacts with the water molecules and its constituents and then re-emerges from the water column without bouncing off from the bottom (Jensen, 2000). It is this portion that has valuable information about the characteristics of the water and its constituents and therefore useful in turbidity analysis (Jensen, 2000, Olet, 2010).

As aforementioned, water turbidity constituents include among others inorganic suspended minerals, organic chlorophyll-*a* and dissolved organic material (Jensen, 2000). Inorganic suspended minerals are a direct consequence of eroded material originating from among others upslope agricultural lands and weathered material (Jensen, 2000). These sediments commonly characterize inland waters and significantly influence spectral reflectance (Jensen, 2000, Miller and McKee, 2004). The presence of these materials affects the absorption and scattering coefficients differently at the various wavelengths. Re-radiated energy is propagated omni-directionally as a function of the size, refractive index and composition of the particles in the solution as well as the wavelength of the incident light (Omar and MatJafri, 2009, Sadar and Engelhardt, Undated). Smaller particles have a greater scattering effect on shorter wavelengths than on longer ones (Sadar, Undated). The reverse holds for larger particles.

2.6.2 Visible and Near-infrared regions

The visible region is reported as most useful in turbidity estimation (Lathrop and Lillesand, 1986, Norsaliza and Hasmadi, 2010b, Wang et al., 2006). Chen and Muller-Karger (2007) note a strong correlation at 645nm using MODIS Terra 250m data. Potes et al. (2012) found the best fit between water turbidity and the green/blue MERIS spectral band index. Interesting features have also been noted in the near-infrared region. This region had previously received little attention due to pure water's high absorption coefficient particularly in longer wavelengths (Doron et al., 2011). However, recent studies have noted that turbid waters, particularly those characterized by inorganic material, display a noticeable degree of reflectance following the presence of minerals (Doxaran et al., 2002, Ruddick et al., 2006, Shibayama et al., 2007). Good results have also been reported in turbidity estimation (Senay et al., 2001; Doxaran et al., 2002).

2.7 Methods of estimating water quality constituents

Existing literature distinguishes between analytical and empirical approaches for estimation of water quality constituents.

2.7.1 Analytical

The analytical approach makes use of bio-optical models, which basically capture the interactions between water and radiation (Koponen, 2006, Wong et al., 2008). This approach makes use of the inherent optical properties (absorption and backscattering) of water bodies to develop models. Once developed and verified, the models can be applied to any dataset regardless of its time of acquisition (Sugihara et al., 1985, Turdukulov, 2003). The main challenges with this approach are the assumption of an even distribution of water quality parameters within the water column, which may not hold in dynamic systems like rivers (Turdukulov, 2003). It also originates from a complicated computational procedure, which hampers its use and understanding.

2.7.2 Empirical

The empirical approach establishes a statistical relationship between the water constituent concentration and reflectance (Turdukulov, 2003). It forges a relationship between recorded spectral data and water quality parameter's *in situ* data using a statistical method that seeks to minimize the error between the variables (Koponen, 2006). It can also be described as a method that utilizes experimental datasets and statistical regression techniques to develop algorithms that relate water-leaving reflectance to *in situ* measurements (Matthews et al., 2010). It is important to note that the development of algorithms requires concurrent acquisition of both *in situ* water quality samples and remote sensing data (Liu et al., 2003). Such synchronization is important in capturing the temporal dynamics of water quality. Resulting statistical relationships can take a simple linear, multiple linear or even non-linear character (Han and Rundquist, 1997, Koponen, 2006, Liu et al., 2003, Turdukulov, 2003). The approach comes with its own pros and cons. The main drawbacks are that it is mostly limited to cases where *in situ* data is available and the resulting algorithms remain sufficient only for that particular dataset from which they were developed (Dekker et al., 1996, Koponen, 2006). This makes them not easily transferable to other areas or across seasons. However, the method is accurate and easy to use (Koponen, 2006, Matthews et al., 2010).

2.8 Algorithm development

The development of algorithms essential for the prediction and estimation of water quality parameters requires statistical applications. There exist a variety of algorithms that are in use today. Some employ simple linear regressions between reflectance and water quality parameters (Koponen, 2006, Turdukulov, 2003, Liu et al., 2003). Others make use of multiple regressions (Ekercin, 2007).

The use of spectral indices in remote sensing studies has become popular since it was first initiated by Kauth and Thomas (1976) (Yamaguchi and Naito, 2003). Indices are very instrumental in converting spectral reflectance at specific wavelengths into biophysical information that can be easily interpreted (Shafique et al., 2003; Koponen, 2006). They essentially enhance the detectability of a particular parameter amongst others (Shafique et al., 2003). They are developed to improve parameter estimates. Several indices have been developed thus far, some for vegetation, soil and water detection. Generally bands, preferably adjacent, carrying the most information about the particular parameter of interest (usually the peaks and troughs of spectral reflectance graphs), are selected (Shafique et al., 2003). This involves analysis of the actual spectral plot for the peaks and troughs. Once the bands of interest have been identified, a series of indices can be derived using arithmetic computations such as band ratios, band differences, first derivatives of bands and/or a combination of ratios and band differences. Examples of these have been reported (Abd-Elrahman et al., 2011, Cairns et al., 1997, Duan et al., 2007, Koponen, 2006, Senay et al., 2001, Turdukulov, 2003, Turdukulov and Vekerdy, 2003, Arenz Jr et al., 1996, Han and Rundquist, 1997, Huang et al., 2010, Kutser et al., 2005, Östlund et al., 2001, Sudheer et al., 2006).

A common example to this is the normalized difference vegetation index (NDVI) first applied by Rouse et al. (1974). Since then many indices, new and modifications of existing ones, have been developed (Haboudane et al., 2004). Literature reports successful spectral indices in turbidity detection. Doxaran et al. (2002) obtained a convincing relationship with turbidity results when the ratio of near-infrared and visible bands was considered. This current investigation made use of these previous findings to guide the current exploration (Chen et al., 2009, Senay et al., 2001, Turdukulov, 2003). A recent addition is the use of derivatives of measured spectra in developing algorithms, which together with band ratios have been considered key in separating spectral effects of different water constituents (Giardino et al., 2007, Han and Rundquist, 1997, Turdukulov, 2003).

Most of these applications have been applied mostly over ocean water where the major optically active constituent is chlorophyll. However, radiation in inland freshwater bodies comprises of complex energy interactions due to the presence of other constituents. This results in considerable scattering and can complicate the relationship between measured spectra and measured constituent's concentrations (Sudheer et al., 2006).

2.9 Summary

Deteriorating water quality is a global problem. Generally, turbidity limits water's utilization value, adds on water treatment costs and induces disease outbreaks. Consequently, turbidity measurement helps monitor water quality which play an important role in detecting the impacts of agricultural and urban sediment loads on water resources. With notable advancements in remote sensing such as spectral improvements, it is now possible to use remote sensing to detect turbidity. Empirical methods that establish a relationship between recorded radiation energy and measured turbidity play an important role in water turbidity detection. However, most of the work done is over ocean waters. Little has been reported on inland freshwater bodies largely due to the complex energy interactions caused by suspended materials. It is therefore important to explore and select optimal spectral bands suitable for turbidity detection.

CHAPTER 3: RESEARCH METHODOLOGY

3.1 Introduction

This chapter details the methods employed in this study to realize the objectives outlined in Chapter 1. It summarizes how spectral reflectance and corresponding turbidity readings were measured at different levels of soil in an amount of water. It also explains the methods of analysis adopted to ascertain answers to the question of optimal spectral bands for turbidity determination.

3.2 Data acquisition and methods

To achieve the set objectives as outlined in Section 1.3, the study selected a suitable area from which soil samples were collected. These were used to create different levels of turbidity through mixing a known amount of soil material in a known volume of water. It was from these mixtures that the respective spectral reflectance together with the corresponding laboratory based turbidity data, were collected. The data collected was analyzed to explore the connection between turbidity and spectral reflectance and also identify optimal spectral bands in turbidity estimation. The methods adopted in data collection and analyses are elaborated upon.

3.2.1 Study area

The soil samples used in this study were localized along the bank of the Msunduzi River in the Pelham area, Pietermaritzburg. The site is gently sloped with minimal topographic variations that are attributed to the river's history of dredging and associated silt deposition (Singh, 2010). The site falls within an area that is currently being used as a recreational park area. There's moderate vegetation cover with a distinct avenue of trees along the river. The river has a turbid character following upstream and surrounding erosion of soil and other contaminants. It flows in a west east direction. To mimic the turbidity characteristics of the river, it was deemed necessary to collect soil sample material close to the river. A locality map, showing the sample points with the latest aerial photograph underlay, was prepared and is presented in Figure 4.

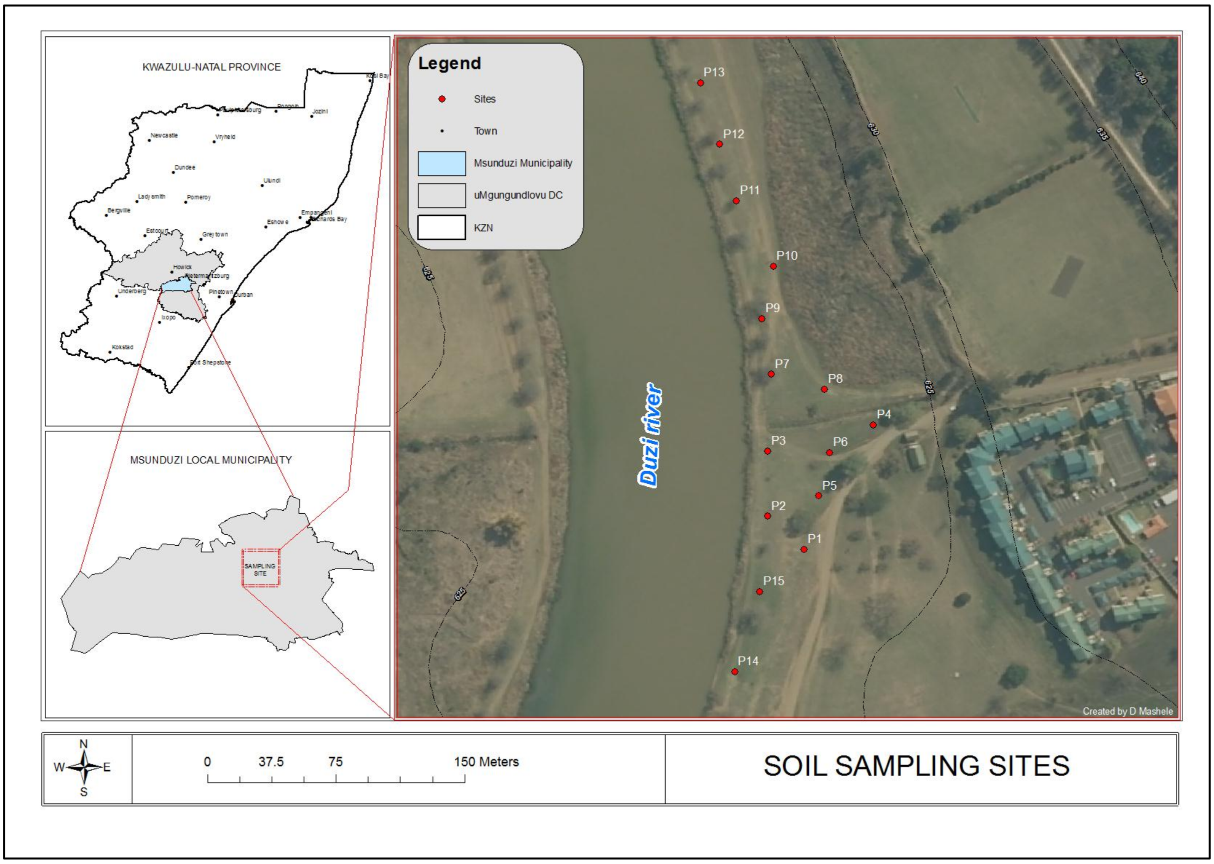

Figure 4: The distribution of sample sites in the study area

3.2.2 Soil samples

Samples were sited using a systematic random sampling approach separated by an approximate distance interval of 40 meters (Figure 4). Since the focus of the study was not on the impact of different soil types in turbidity but rather on the amount, the siting of the sample sites at specified distances was meant for data separability not soil type differences. An approximate mass of 3 kilograms of soil was collected at each of the 15 sampling sites and then oven dried over night at 105^{o}C. This temperature is recommended as it does not alter the chemical and physical attributes of the soil (Carter and Gregorich, 2008). After drying, the collected samples were gently crushed and passed through a 2mm diameter mesh sieve. The sieved soil samples served as input for the turbid solutions from which both the laboratory and spectral reflectance measurements were performed. Using an electronic scale, 15 different mass levels incremented by 10 grams (g) (i.e 10g, 20g, 30g…150g) were weighed out from each sieved soil sample. Weighing these samples was important in creating solutions of different turbidity levels. The resulting masses were secured in sealable plastic bags. This exercise generated a total of 225 soil replicates, 15 for each mass level. An approximate mass of 460g from each sample was taken to the Department of Agriculture and Environmental Affairs in Cedara, KwaZulu-Natal for determination of chemical and physical characteristics (Table 2).

3.2.3 Spectral measurements of turbid solutions

The 255 weighed sieved soil masses were used to prepare turbid solutions upon which the spectral measurements were to be conducted. Spectral reflectance data was collected using a 350 to 2500nm Analytical Spectral Device (ASD) field spectroradiometer (FieldSpec®, Analytical Spectral Devices, Inc., US) in the field. The ASD device records radiation at 1.4-nm intervals and 2-nm intervals for the spectral regions 350 to 1000 nm and 1000 to 2500 nm, respectively. Data were interpolated to 1-nm spectral resolution across the spectrum. To minimize bi-directional influence as per changing sun angle, measurements were taken under clear sunlight between 10 am and 14 pm. Prior to data collection, the spectrometer was calibrated to respective spectral measurement lighting conditions using a Spectralon white reference panel. The validity of the calibration was tested using the panel's reflectance. During spectral measurement, calibration was repeated after an average of 30 spectral scans were collected or when the instrument reached saturation. Care was taken not to handle or expose the panel to dirt, water or any other damaging substance during and after calibration.

Two 1000 milliliters glass beakers of 10.5 cm diameter and 14.5 cm depth were used to hold samples for spectral measurements. The first beaker was wrapped with a black plastic liner so as to limit light interference from the surroundings (Lodhi et al., 1997, Karabulut and Ceylan, 2005). The second beaker was unlined and used to mix the different turbid concentrations. Each sieved soil mass increments (i.e 10 to 150g) was transferred into the unlined 1000ml glass beaker, one at a time, together with a litre of deionized water and stirred to make a turbid solution. Deionized water was preferred so as to minimize the possible influence of any dissolved salts in water on the reflectance. The solution was then transferred into the lined beaker, filling it up to the 1000ml mark with the solution, for spectral measurements. The sediment was kept in suspension by manually stirring so as to ensure the homogeneous distribution in the water. The solution was given a brief delay prior to scanning to avoid wave effects. Once ready the 1 degree field of view (FOV) head attached to a fibre optic pistol was positioned at about 10cm directly above the water surface and the spectral reflectance measurement taken. To avoid spectral contamination, care was taken to ensure that only the spectral reflectance of the water solution covered by the FOV was recorded. An average of 15 scans ranging from 350-2500nm wavelength range within the electromagnetic spectrum was taken. The spectral reflectance of deionized water (0 g/l) was also collected so as to quantify the signature of pure water. The same procedure was followed to record the spectral reflectance of the rest of the prepared turbid solutions at the different concentration levels (10g/l, 20g/l, 30g/l, 40g/l, 50g/l, 60g/l, 70g/l, 80g/l, 90g/l, 100g/l, 110g/l, 120g/l, 130g/l, 140g/l and 150g/l).

3.2.4 Laboratory turbidity measurements

The laboratory based turbidity measurements were carried out using a 2100Q portable turbidimeter (Hach Company. Loveland, Colorado). This instrument makes use of a tungsten filament lamp source and a silicon photodiode detector to determine the amount of particles in the solution. After an initial calibration, the turbidity measurement is achieved by turbidimetric ratio determination using a primary nephelometric light scatter signal positioned at 90^{o} to the transmitted light scatter signal. Typically, the device is battery powered with a measurement range of 0 to 1000 Nephelometric Turbidity Units (NTU). It has a resolution of 0.01 NTU and an accuracy of ±2% of reading plus stray light (≤ 0.02). Due to instrument unavailability, the turbidity measurements were sourced out to a nearby water testing agency, Talbot & Talbot (Pty) Ltd. As part of the agency's regulation, a volume of 500ml of the turbid solution is required for turbidity measurements. This ensures that analyses can be repeated if and when errors are encountered.

Laboratory based turbidity measurements were carried out from the same type of turbid solutions created from mixing each of the weighed sieved masses with deionized water, thus creating turbid solutions of different concentrations as in Section 3.2.3. These were thoroughly mixed and then half the solution (500ml), as required by the water testing agency, transferred into 500ml sealable plastic bottles to be sent for laboratory analysis. It is noted though that due to the project's limited funds only 149 out of the 255 prepared turbid solutions was analyzed for laboratory turbidity (see Table 2). This number covers approximately 11 of the primarily 15 initially collected soil samples.

Prior to analyses, the agency subjected each of the 500ml solutions to gentle shaking to facilitate homogeneity. From these solutions, 15ml aliquots were extracted using a sample cell from which the turbidity values were to be measured. A thin film of silicon oil was applied over the entire surface of the sample cell to mask the sample cell's minor imperfections and scratches that may contribute to light scattering. Thereafter the turbidity values were measured from the extracted 15ml aliquots within 24 hours of mixing to minimize the influence of any possible organic or chemical reactions, and then measured data transferred into an MS excel spreadsheet and basic statistics computed. In cases where the turbidity value exceeded the instrument's high limit (i.e 1000 NTU), the extracted aliquots would be diluted with Type 1 Milli-Q water (ultrapure grade water) to acceptable ratios, then the turbidity would be measured from the resulting solution and the resulting value multiplied by the factor of dilution to get the turbidity value of the original solution.

3.3 Processing

3.3.1 Initial spectra processing

Using the ViewSpec Pro™ spectra viewing software, the collected spectra were explored and mean spectra at each wavelength computed. The computed files were converted into ASCII text files readable in MS Excel. The spectral range was limited between 400 to 1000 nm firstly because noise became a problem at wavelengths beyond this spectral range. Secondly, literature reports this range as the most appropriate for turbidity detection (Norsaliza and Hasmadi, 2010a, Senay et al., 2001, Wang et al., 2006). It was also noted that water displays interesting spectral responses in the said range, particularly the near-infrared region and therefore the study sought to investigate its relevance to turbidity detection. Reflectance was computed as the ratio between reflected energy from the water surface and the Spectralon white reference panel.

3.3.2 Estimating turbidity

The relationships between the raw spectral reflectance in the 400 to 1000nm range and laboratory based turbidity measurements were tested using the Pearson's coefficient of correlation (r) with a significance of $p<0.05$. The test yielded poor results with its highest coefficient being 0.4. The study therefore opted to compute the mean spectral reflectance (denoted by X10 to X150) at each of the turbid solution' concentration level (i.e. 10g/l up to 150g/l). This helped compensate against noise and also enhanced variability between the different turbidity levels.

The resulting spectra were explored for the strongest and most appropriate band/s per spectral portion (i.e. blue, green, red and near-infrared) in turbidity detection using Pearson's coefficient and simple regressions. It was important to partition the bands according to their "natural" regions because of their unique characteristics and behavior in water. Jensen (2000) explains the roles of the different regions, pointing out the usefulness of the visible and near-infrared regions in providing information about the type of soil and amount in suspension, respectively. This partitioning helped reduce the probability of selecting bands containing the same information (i.e. data redundancy) as a result of inter-band correlation. The study also explored for optimal spectral indices using the same criteria as single bands above. As mentioned in Section 2.8, spectral indices enhance the detectability of a particular parameter and also improve parameter estimates (Shafique et al., 2003). The exploration involved first derivatives of reflectance, band differences, band ratios and combination indices. Their associated formulae are presented in Table 1. Most of the indices explored were traced from previous turbidity studies.

Table 1: Formulae for spectral indices

Index type	Computation	References
Simple ratio	R_i / R_j	Koponen (2006), Shafique et al. (2003), Potes et al. (2012)
First derivative	$(R_i - R_j) / (\lambda_i - \lambda_j)$	Senay et al. (2001)
Band differences	$R_i - R_j$	Shafique et al. (2003)
Normalized indices	$(R_i - R_j) / (R_i + R_j)$	Shafique et al. (2003)

where R_j and R_i represent the spectral reflectance at band i and j, and λ_i and λ_i are the band wavelengths at band i and j.

Using regression analysis, the best bands, per spectral portion (blue, green, red and near-infrared), were selected noting their respective Pearson's coefficient of correlation and the resulting coefficient of determination (R^2) with measured water turbidity. Bands that yielded the highest R^2 values against turbidity constituted the best bands. The study selected the best 3 bands, as informed by Mutanga and Rugege's (2006) method, from each spectral category (i.e. blue, green, red and near-infrared), and using the highest R^2 criteria after cross validation as explained below, the best band, in each spectral category, was noted. These are also treated as representative bands for each of the spectral categories. There was a slight variation in the near-infrared region. An additional band was included in this category, thereby making a total of 4 bands. The reason behind the additional band is informed by the wideness of the near-infrared region. It was observed that one end of the region is dominated by high reflectance while the other by low reflectance (see Figure 7). It was therefore interesting to see how these differences would impact the strength of the relationship with turbidity. Furthermore, 2 spectral indices, one from each region (i.e. visible and near-infrared), were selected. In the end a total of 13 best single bands plus 2 spectral indices were extracted, thereby making a total of 15 variables.

3.3.3 Model validation

The usefulness of values estimated with remote sensing is very limited without proper indications of their accuracy. The study computed regression models between the observed and predicted values of turbidity and then subjected resulting models to a validation process using the leave-one-out cross-validation (LOOCV) procedure. The LOOCV technique isolates a single observation for validation purposes and then uses the rest of the observations as training data. This was done for all of the observations. The resulting model was then used to predict the previously isolated observation. In each iteration, adjusted R^2 and root mean square error (RMSE) values were recorded and later the mean values of each computed. The RMSE value and the adjusted R^2 were calculated by relating the predicted value generated during the LOOCV procedure to the observed value so that the accuracy of turbidity estimation can be ascertained. The technique is widely used in remote sensing and well suited for small sample sizes (Wang et al., 2013, Sterckx et al., 2007). Models with the highest R^2 and the lowest RMSE were considered as optimal.

3.4 Summary

A total of 15 soil samples were collected in the study site, oven dried, sieved and replicates extracted. The replicates, with masses ranging from 10 to 150g, were each mixed with deionized water to create turbid solutions over which spectral reflectance together with laboratory based turbidity values were measured. The basic soil chemical and physical characteristics were also determined. Thereafter, the spectral data was explored for the strongest relationships with measured turbidity and then R^2 value reported. Models were cross validated using the LOOCV procedure, reporting both the RMSE and adjusted R^2.Such exploration was limited to the visible-near infrared region of the spectrum. A few spectral bands displayed strong relationships with turbidity.

CHAPTER 4: RESULTS

4.1 Introduction

As set out in Chapter 1, this study sought to investigate the relationship between turbidity levels and spectral reflectance and then move on to identify the optimal bands that can be used to estimate turbidity. Consequently, this chapter presents results from the soil analysis, laboratory based turbidity measurements, spectral reflectance measurements and the investigation to identify optimal bands that correlated best with turbidity measurement.

4.2 Soil properties and reflectance

Soil attributes play a significant role in the amount of electromagnetic energy reflected or absorbed (Rossel et al., 2006). Demattê et al. (2010) note a close relationship of soil attributes such as organic matter with reflected energy. Other studies have explored this connection by using visible near-infrared spectroscopy to predict organic carbon, nitrogen, clay content, exchangeable calcium, micronutrients and others (Bilgili et al., 2010). Jensen (2000) notes a distinction in reflectance between silty and clayey soil, reporting higher reflectance values in the visible region for silty soils in comparison to all other wavelength regions.

The soils used in this study were predominantly clay loam, darker in colour with a significant amount of organic matter and clay (Table 2). There was little variation in soil attributes as sampling was localized around the same area.

Table 2: Physical and chemical properties of soil samples used

	Mean	Median	Min	Max	Variance	Std.dev
Clay %	34.667	35.000	29.0000	38.000	6.2	2.4976
Fine Silt %	25.467	26.000	20.0000	28.000	4.1	2.0307
Coarse Silt & Sand %	40.267	39.000	34.0000	51.000	19.6	4.4315
Total % Nitrogen	0.216	0.220	0.1300	0.330	0.0	0.0497
Total % Carbon	2.537	2.590	1.9100	3.600	0.2	0.4420
Sample density (g/ml)	1.085	1.100	0.9800	1.160	0.0	0.0427
P (g/ml)	6.467	6.000	2.0000	17.000	16.3	4.0332
K (g/ml)	191.133	184.000	101.0000	435.000	6945.6	83.3400
Ca (g/ml)	1658.200	1915.000	172.0000	1968.000	369170.9	607.5943
Mg (g/ml)	729.400	730.000	665.0000	813.000	1443.5	37.9940
Ex acidity (cmol/L)	0.080	0.080	0.0400	0.130	0.0	0.0251
Total cations (cmol/L)	14.845	15.970	7.5400	16.700	7.8	2.7927
Acid sat %	0.600	1.000	0.0000	1.000	0.3	0.5071
Ph (KCl)	5.094	5.090	4.9600	5.370	0.0	0.1175
Zn (g/ml)	10.287	7.200	4.4000	60.800	197.6	14.0567
Mn (g/ml)	135.600	120.000	44.0000	250.000	2573.3	50.7273
Cu (g/ml)	6.927	6.900	5.8000	7.800	0.4	0.6262
Organic C %	2.013	1.900	1.6000	2.900	0.1	0.3441
N %	0.203	0.210	0.1600	0.280	0.0	0.0315

4.3 Turbidity

The study used the average values of laboratory based turbidity measurements in each concentration level (i.e. X10 to X150). Computed statistical attributes of turbidity data are presented in Table 3. The data depicted a predominantly normal distribution as shown in Figure 5 below. It is noted that Table 3 contains values that exceed the 1000 NTU instrument’s high limit. Such values were possible through the use of the dilution method explained in Section 3.2.4 above. Turbidity measurements at X140 and X150 are lower than expected. This is possibly a result of outliers or human error during data transfer at the testing agency.

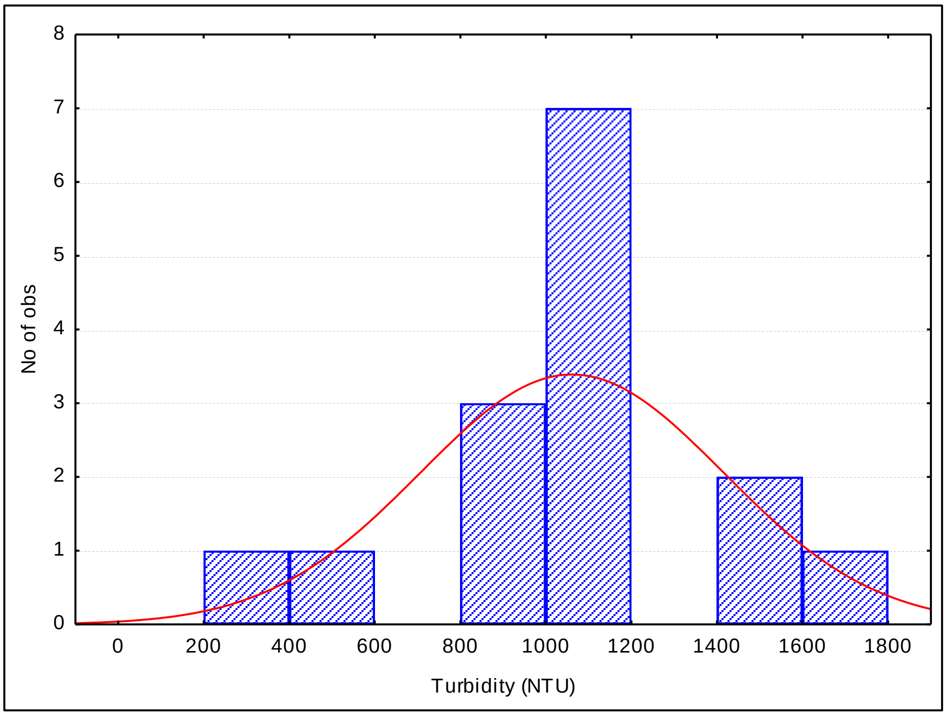

Figure 5: Laboratory based turbidity data distribution

Table 3: Descriptive statistics of measured turbidity (in NTU)

Sample	No. of sample	Mean	Median	Minimum	Maximum	Variance	Std.Dev.
X10	11	302.545	288.000	106.0000	590.000	21044	145.066
X20	10	471.900	486.000	153.0000	676.000	31287	176.883
X30	11	837.909	722.000	229.0000	1546.000	178824	422.876
X40	10	899.700	759.500	272.0000	1582.000	228842	478.374
X50	10	1037.100	896.500	524.0000	1924.000	232300	481.975
X60	10	1146.600	770.000	486.0000	2912.000	678914	823.962
X70	10	1107.200	932.500	442.0000	2850.000	492790	701.990
X80	10	1442.200	1341.000	389.0000	2984.000	629302	793.286
X90	10	1178.200	1053.000	403.0000	2684.000	495174	703.686
X100	10	1005.900	862.500	277.0000	2420.000	447225	668.749
X110	10	1121.500	934.000	108.0000	2310.000	624012	789.944
X120	10	1510.900	1027.000	442.0000	3900.000	1277542	1130.284
X130	9	1660.333	934.000	530.0000	7180.000	4401378	2097.946
X140	9	981.000	990.000	542.0000	1506.000	95724	309.393
X150	9	1125.556	1322.000	461.0000	1922.000	308704	555.611

As shown in Figure 6, there was a positive relationship between measured turbidity and the amount of soil in water.

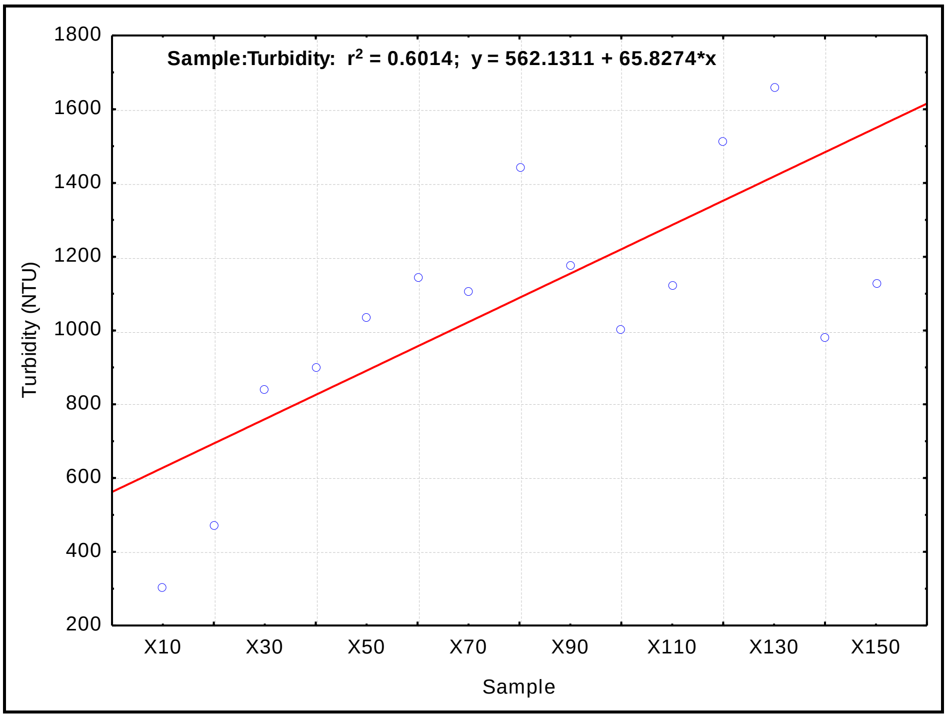

Figure 6: Average laboratory based turbidity measurements against amount of soil in solution.

4.4 Spectral characteristics of different turbidity levels

Figure 7 depicts the different general spectral responses of clear and turbid waters. As shown in the figure clear water displayed a “normal” spectral reflectance dome shape. Clear water reflected high around the visible region and also displayed an almost total absorption in the longer near-infrared wavelengths. Turbid water, across all levels (i.e. X10 to X150), displayed low reflectance below 420 and above 930nm. Four significant reflectance peaks were noted, two in the visible region at around 450 and 580nm, and the other two in the near-infrared region at 751 and 771nm. A series of troughs caused by atmospheric and water absorption were noted at bands 655, 687, 718 and 761nm. The most pronounced absorption occurs in the 761nm band which falls in the near-infrared region. These areas are encircled red in Figure 7 below. It is noted that these areas were excluded from the optimal band exploration.

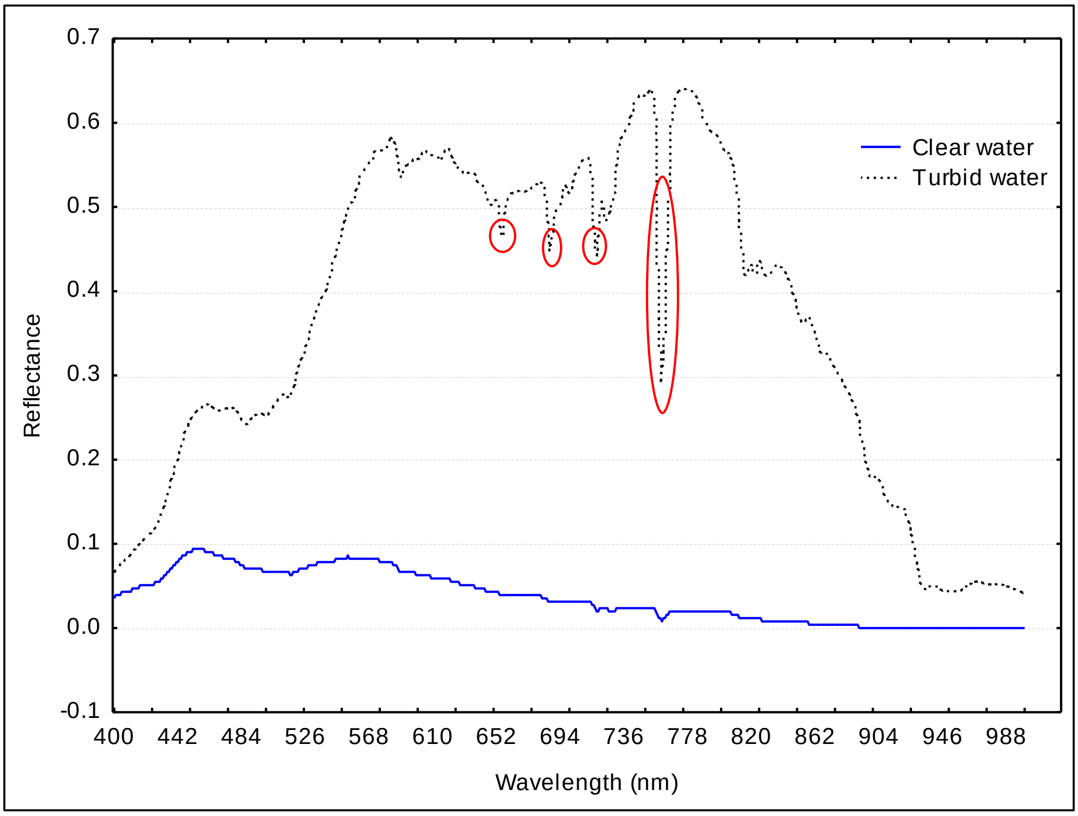

Figure 7: A general spectral reflectance characteristic of turbid and clear water with absorption bands (highlighted in red)

The impact of the amount of suspended material in solution is captured in Figure 8. A general increase in reflectance as one move from clear water to slightly turbid and to strongly turbid solutions, depicted by X10 to X150, is evident. Differences in reflectance are more pronounced at low levels than at high levels. These results are consistent with Moore (1980) who notes that turbid systems reflect more energy than clear ones as a result of suspended material.

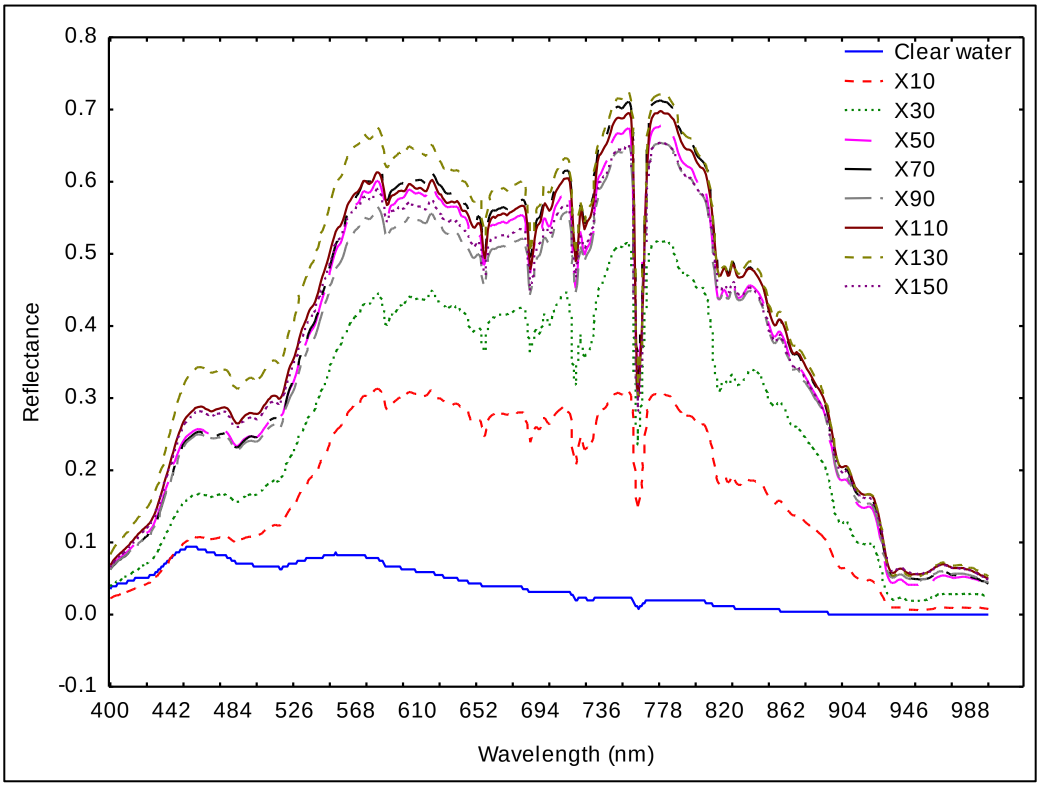

Figure 8: Spectral reflectance of solutions with varied amounts of soil

4.5 Optimal bands

4.5.1 Visible region

Using the Pearson's coefficient of correlation and simple regressions, the relationships between the 301 spectral bands in the visible region and increasing turbidity were tested. As described in Chapter 3.3.2, the best 3 bands in each spectral category were extracted and are presented in Table 4.

Table 4: Visible region bands

Spectral category	Band (nm)	r-value	R^2
GREEN	520	0.840753	0.7069
	521	0.840626	0.7067
	528	0.841583	0.7083
BLUE	489	0.838033	0.7023
	490	0.837457	0.7013
	491	0.837411	0.7013
RED	657	0.829897	0.6887
	659	0.829474	0.6880
	658	0.829203	0.6876

These bands went through the process of cross validation so as to assess their accuracy. Results from the process are presented in Table 5 below. Of the 9 bands selected in the visible region, bands 528, 489 and 657 yielded the lowest RMSE values and highest adjusted R^2 values in their respective spectral categories. These were treated as representatives of each of the band categories considered in the visible region and have been presented in Figures 9 to 11 below. It is noted that they all characterize a positive trend with increasing reflectance

Table 5: LOOCV results of visible bands

Band	***Mean adjusted R^2***	***Mean RMSE (in NTU)***	***RMSE %***
528	0.7062	182.4267	17.3
520	0.7049	182.8043	17.3
521	0.7047	182.8711	17.3
489	0.7004	184.1968	17.5
490	0.6995	184.4922	17.5
491	0.6994	184.5103	17.5
657	0.6864	188.9770	17.9
659	0.6857	189.1897	17.9
658	0.6853	189.3202	17.9

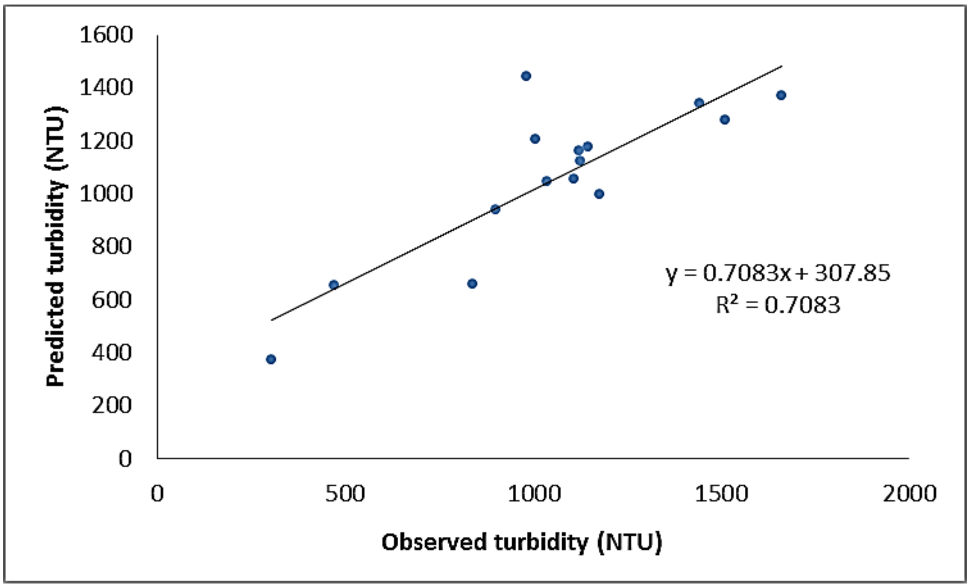

Figure 9: Regression model of observed and predicted turbidity at 528nm

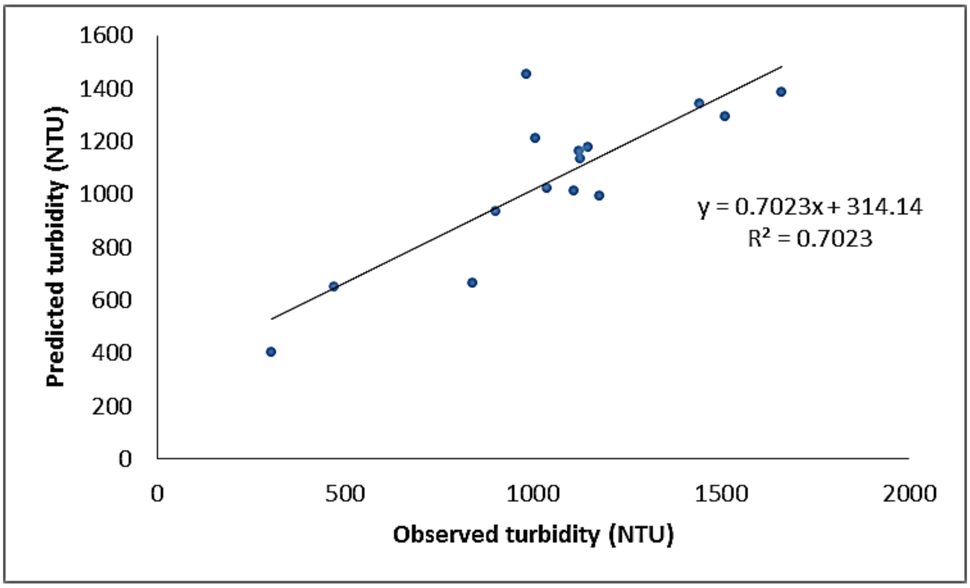

Figure 10: Regression model of observed and predicted turbidity at 489nm

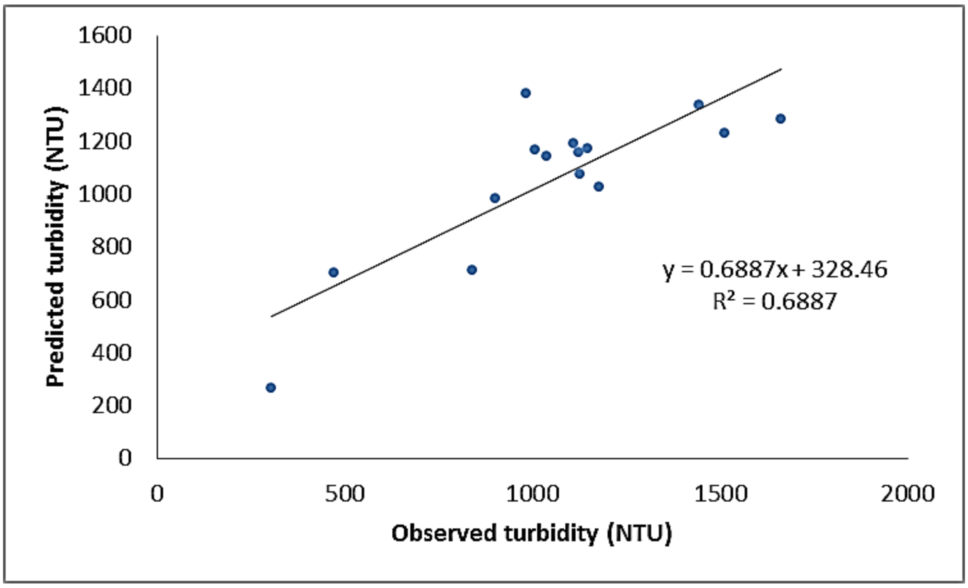

Figure 11: Regression model of observed and predicted turbidity at 657nm

4.4.2 Near-infrared region

The definition and selection of the best band in this region used the same criteria outlined in Section 3.3.2 above except that the best 4 instead of 3 were selected. As explained earlier, this was because of the near-infrared unique high and low reflectance ends. The selected bands are presented in Table 6.

Table 6: Near-infrared region optimal bands

Spectral category	Band (nm)	r-value	R^2
Near-infrared	1000	0.845278	0.7145
	983	0.835728	0.6984
	868	0.834331	0.6961
	766	0.819656	0.6718

The near-infrared region displayed strong agreement between predicted and observed turbidity values at bands 1000 and 983nm yielding 0.7145 and 0.6984 respectively (Figures 12 and 13).

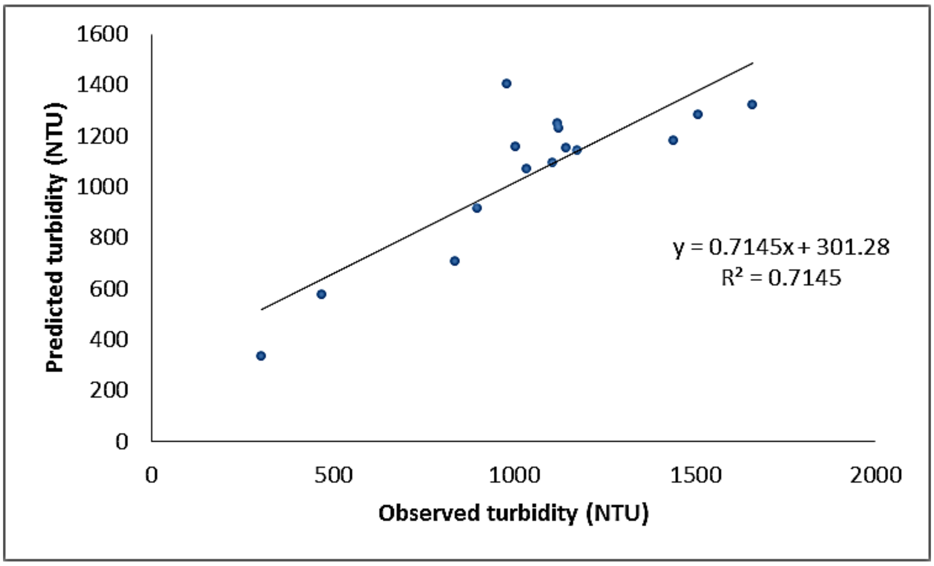

Figure 12: Regression model of observed and predicted turbidity at 1000nm

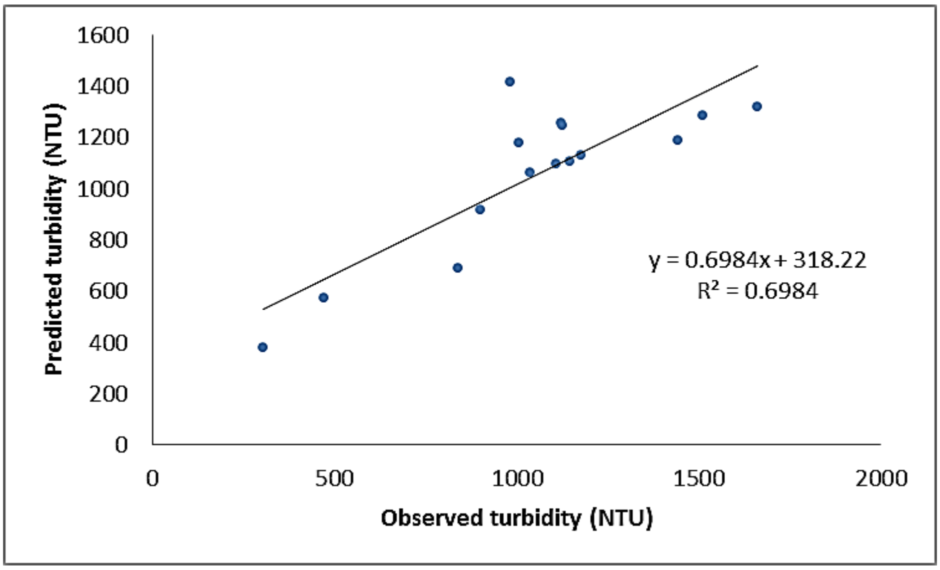

Figure 13: Regression model of observed and predicted turbidity at 983nm

The results above are surprising because near-infrared wavebands have always been associated with zero water-leaving reflectance (Dogliotti et al., 2011). However, reports have previously been made about some usefully measureable energy found in the longer wavelengths of the incident light scattered by suspended particles in the very thin layer at the water surface (Shibayama et al., 2007). This investigation was able to detect some of this energy.

The validation process yielded an error of less than 20% of the mean observed turbidity values in all selected bands. Table 7 summarizes the validation process results reporting the mean adjusted R^2 and RMSE values.

Table 7: LOOCV results of near-infrared bands

Band	***Mean adjusted R^2***	***Mean RMSE (in NTU)***	***RMSE %***
1000	0.7120	180.8223	17.1
983	0.6961	185.7827	17.6
868	0.6944	186.6680	17.7
766	0.6700	194.0762	18.4

4.4.3 Spectral indices

As aforementioned, the use of spectral indices is largely motivated by the need to improve turbidity estimation. The study tested over 30 indices as reported in literature for turbidity detection. These included spectral ratios, differences, first derivatives and combination of ratios and differences based on formulae in Table 1. The spectral indices are presented in Table 8 below.

Table 8: Tested spectral indices ranked according to R^2 (significant at $p<0.05$)

Rank	Band ratio/index	r	R²	p
1	(770-1000)/(770+1000)	-0.837	0.700	0.000100
2	625/440	-0.828	0.685	0.000140
3	(560-520)/(560+520)	-0.827	0.684	0.000143
4	774-905	0.826	0.682	0.000148
5	894-905	0.823	0.677	0.000166
6	460/540	0.820	0.672	0.000184
7	450/600	0.818	0.670	0.000192
8	770-975	0.816	0.666	0.000209
9	770/1000	-0.815	0.664	0.000217
10	441.4 / 640.8	0.809	0.655	0.000257
11	748-870	0.809	0.655	0.000259
12	677/488	-0.808	0.653	0.000267
13	540-460	0.807	0.651	0.000280
14	710-740	-0.805	0.648	0.000294
15	(760-905)/(760+905)	-0.799	0.639	0.000350
16	490/670	0.794	0.630	0.000409
17	800/900	-0.788	0.621	0.000484
18	450/520	0.784	0.614	0.000547
19	(800-900)/(800+900)	-0.778	0.606	0.000632
20	900-970	0.778	0.605	0.000639
21	(774-905)/(774+905)	-0.771	0.594	0.000765
22	765/865	-0.762	0.581	0.000960
23	625 - 440	0.759	0.575	0.001045
24	748/870	-0.748	0.559	0.001348
25	710/740	-0.718	0.516	0.002559
26	(710-740)/30	-0.718	0.516	0.002559
27	710/720	-0.658	0.433	0.007643
28	702/740	-0.630	0.397	0.011863
29	710-720	0.600	0.360	0.018041
30	(765-865)/100	0.551	0.304	0.033255
31	(675-700)/25	-0.431	0.186	0.108324
32	(700-675)/25	0.431	0.186	0.108324
33	760-905	0.395	0.156	0.145504
34	802/798	-0.387	0.150	0.154252

Of all the tested indices only the best two (2) were selected. These were ratios 625/440 and (770-1000)/(770+1000), with R^2values of 0.685 and 0.70 respectively. Figures 14 and 15 depict the resulting regression models for turbidity estimation.

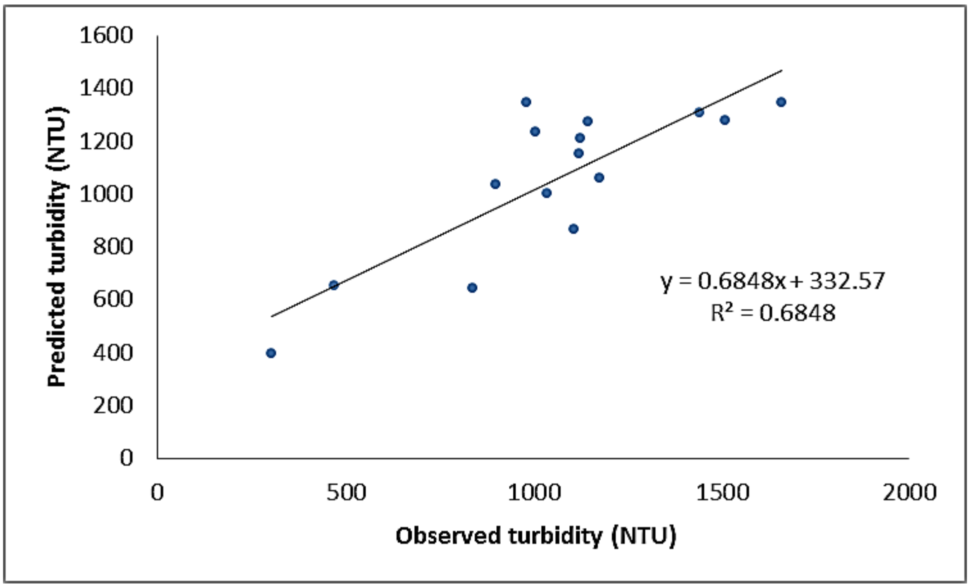

Figure 14: Regression model of observed and predicted turbidity at 625/440

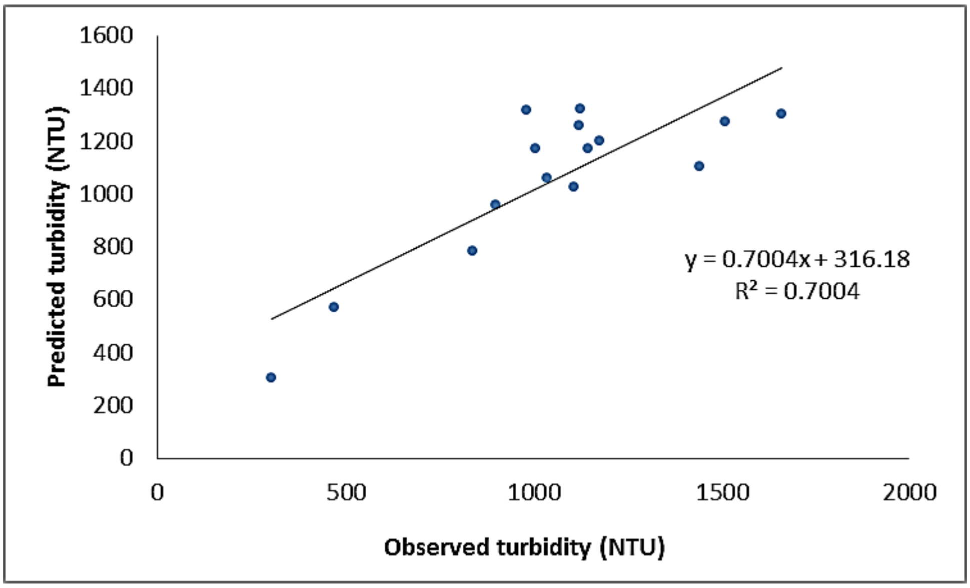

Figure 15: Regression model of observed and predicted turbidity at (770-1000) / (770+1000)

The 625/440 ratio combines spectral attributes of the red and blue categories which are deemed useful to turbidity studies. A similar combination yielded good results in Ouillon et al. (2008), producing the highest R^2 value with turbidity. The 700-1000/770+1000 index produced the highest R^2 value of all tested indices. This index normalizes the reflectance between 770 and 1000nm. It combines bands of highest and lowest reflectance from the actual data. A R^2 value of 0.70 shows a significant connection with turbidity. These models were also subjected to a validation procedure as in the previous occasion in Section 4.4.1. Both models returned an error that is less than 20% of the mean turbidity observations, which indicates good model performance (Table 9).

Table 9: LOOCV results of selected spectral indices

Band	***Mean adjusted R^2***	***Mean RMSE (in NTU)***	***RMSE %***
625/440	0.6822	190.2477	18.0
770-1000/770+1000	0.6973	185.6616	17.6

CHAPTER 5: DISCUSSION AND CONCLUSION

5.1 Introduction

The use of hyperspectral data in water quality studies comes with great benefits and opportunities like minimizing costs, time and resources needed on one hand and revealing important implicit relationships and characteristics about features on the other. Water turbidity is characteristic of South African rivers due to the coincidence of an arid climate and high intensity rainfalls (Dörgeloh, 1995; Dörgeloh et al., 1993). It remains an important measure of river health and landscape-transforming processes, presenting a great opportunity into which hyperspectral data can be applied. Challenges associated with using hyperspectral data encompass the problem of high dimensionality and related multicollinearity. Despite these challenges, spectral data have been successfully applied in turbidity studies (Doxaran et al., 2002; Potes et al., 2012; Chen and Muller-Karger, 2007). The visible and near-infrared regions are particularly useful for turbidity discrimination and estimations, due to the unique interaction of water and inorganic materials with radiation energy.

The current investigation demonstrated the significance of the visible and near-infrared regions of hyperspectral data in turbidity detection. It illustrated the variability of reflectance over water with different levels of sediment concentration. It further highlighted the positive relationship between sediment load and turbidity, forging a clear connection between reflectance and turbidity. Although previous studies established valuable empirical algorithms, most of them employed broad spectral bands that conceal important implicit spectral features (Alcântara et al., 2009, Chen et al., 2007a, Hellweger et al., 2007, Petus et al., 2010, Koponen et al., 2002). It was therefore the object of the investigation to select the optimal bands within the visible near-infrared region in turbidity detection using hyperspectral data.

A total of 13 single bands (520, 521, 528, 490, 489, 491, 658, 657, 659, 1000, 766, 868 and 983nm) plus 2 indices, 625/440 and (770-1000)/(770+1000), were extracted from the 601 bands in the 400-1000nm spectral range as having the strongest relationships with turbidity. The accuracies of the selected bands were tested through the use of the leave-one-out cross validation procedure using the RMSE. Bands 520, 489 and 657 in the visible region yielded the highest adjusted R^2 values and lowest RMSE values in their respective categories and therefore served as categories' representatives. It was interesting to note that the highest coefficient came from band 528, which borders the blue and green categories of the spectrum, with the latter largely associated with chlorophyll-*a*, a parameter with distinct absorption in the blue and red bands (Senay et al., 2001). However, some studies have acknowledged the usefulness of the green band in turbidity quantification (Akbar et al., Undated, Khorram et al., 1991). The 489 and 657 bands are not surprising as they fall within band categories that have already been reported as sensitive to turbidity variation (Lathrop and Lillesand, 1986, Norsaliza and Hasmadi, 2010a). Some report the red band as best correlated with turbidity (Hellweger et al., 2007). A strong linear association between the red and blue (625/440) ratio is consistent with findings from a previous study (Lodhi, 2002).

The strongest relationship was located in the near-infrared region. This region, as previously alluded, makes little contribution in reflectance over clear water as almost all radiation is absorbed. However, the presence of suspended materials alters the water's spectral signature through scattering causing significant reflectance (Doron et al., 2011). Shibayama et al (2007) reported the existence of some usefully measureable energy found in the longer wavelengths that may be scattered by suspended particles in the very thin layer at the water surface. Although not as prominent as the in the visible region, the reflected energy from this region may carry unique additional information. Such attributes have led to it being strongly suggested in turbidity detection (Matthews, 2011). Senay et al. (2001) reports this range, 800-1000nm, as part of the good estimators of turbidity. Also the fact that radiation from this region is able to penetrate the water and interact with the constituents of the water before being recorded by the sensor makes it a reliable measure of water turbidity. It is not too surprising therefore that the strongest relationship with turbidity is located in the region. This is an interesting finding as it amplifies the importance of the subsurface volumetric radiance (L_v) portion of electromagnetic radiation in turbidity detection. It also emphasizes Jensen's (2000) observation about near-infrared region's usefulness in determining the amount of suspended material in water. This observation would consequently prompt further investigation of both theoretical and experimental approaches in the use of near-infrared band in parameter estimations. However, caution should be taken against multiple backscattering in highly turbid systems, particularly in this region, as it may exaggerate the reflectance, yielding misleading results.

Band 983 showed much higher reflectance compared to the 1000nm but yielded slightly lower R^2 value. What is evident from the results is that the near-infrared region remains an important portion of the spectrum in turbidity studies. It is believed that bands from this region contain valuable in-water constituents' information due to their elaborate interaction with in-water constituents.

The cross validation process yielded RMSE values that are less than 20% of the mean turbidity observations. This clearly indicates good performance in the constructed models.

5.2 Conclusion

What can be drawn from this study is firstly that water turbidity is spectrally active and can therefore be interrogated through remote sensing. Secondly, there is a strong connection between the amount of suspended materials, particularly inorganic constituents, and resulting turbidity measure. The presence of such materials induces a reflective character on water through light scattering and backscattering. This phenomenon is very pronounced in the visible and near-infrared regions of the spectrum.

The use of hyperspectral data in turbidity detection is ideal for optimal band interrogation. It offers us the opportunity to fine-tune our understanding of the processes, behaviors and characteristics of spectrally active features, particularly those that play significant role in human livelihood such as water. The bands 528, 489, 657, 1000 and 983 and the two spectral ratio indices 625/440 and (770-1000)/(770+1000), present a strong case in turbidity detection. They boast RMSE values that are less than 20% of the mean measured value in turbidity which means that the models will be accurate 80% of the time. This is an acceptable compromise and therefore the models are highly recommended as starting points for further investigations. Of all the results that this study generated, the ones from the near-infrared region of the spectrum raise much interest. This is largely because this region has often received little attention in turbidity detection because of its pronounced absorption in water. The study therefore recommends further exploration on the role of the near-infrared region in turbidity detection particularly using hyperspectral data.

REFERENCES

ABD-ELRAHMAN, A., CROXTON, M., PANDE-CHETTRI, R., TOOR, G., S, SMITH, S. & HILL, J. 2011. In situ estimation of water quality parameters in freshwater aquaculture ponds using hyperspectral imaging system. *ISPRS Journal of Photogrammetry and Remote Sensing,* 66**,** 463-472.

ADAM, E., MUTANGA, O. & RUGEGE, D. 2010. Multispectral and hyperspectral remote sensing for identification and mapping of wetland vegetation: a review. *Wetlands Ecological Management,* 18**,** 281-296.

AGHIGHI, H., ALIMOHAMMADI, A., SARADJIAN, R. M. & ASHOURLOO, D. 2008. Estimation of water turbidity in Gorgan Bay, South-East of Caspian Sea by using IRS-LISS-III images. *Pakistan Journal of Biological Sciences,* 11**,** 711-718.

AKBAR, T. A., HASSAN, Q. K. & ACHARI, G. Undated. A Remote Sensing Based Framework for Predicting Water Quality of Different Source Waters. *The International Archives of the Photogrammetry, Remote Sensing and Spatial Information Sciences,* 34.

ALCÂNTARA, E., BARBOSA, C., STECH, J., NOVO, E. & SHIMABUKURO, Y. 2009. Improving the spectral unmixing algorithm to map water turbidity Distributions. *Environmental Modelling and Software,* 24**,** 1051-1061.

ARENZ JR, R. F., LEWIS JR, W. M. & SAUNDERS III, J. F. 1996. Determination of chlorophyll and dissolved organic carbon from reflectance data for Colorado reservoirs. *International Journal of Remote Sensing,* 17**,** 1547-1566.

ASHTON, P. J. 2007. Riverine biodiversity conservation in South Africa: current situation and future prospects. *Aquatic Conservation: Marine and Freshwater Ecosystem,* 17**,** 441–445.

BACKEBERG, G. R., BEMBRIDGE, T. J., BENNIE, A. T. P., GROENEWALD, J. A., HAMMES, P. S., PULLEN, R. A. & THOMPSON, H. 1996. Policy proposal for irrigated agriculture in South Africa.

BERNSTEIN, S. Undated. Freshwater and Human Population: A Global Perspective. *Human Population and Freshwater Resources.* Yale F & ES Bulletin.

BHATTI, A. M., NASU, S. & TAKAGI, M. 2007. Assessment of Suspended Sediment Concentration in the Surface Water Using Remote Sensing.

BIERMAN, P., LEWIS, M., OSTENDORF, B. & TANNER, J. 2011. A review of methods for analysing spatial and temporal patterns in coastal water quality. *Ecological Indicators,* 11**,** 103-114.

BILGILI, A. V., VAN ES, H. M., AKBAS, F., DURAK, A. & HIVELY, W. D. 2010. Visible-near infrared reflectance spectroscopy for assessment of soil properties in a semi-arid area of Turkey. *Journal of Arid Environments,* 74 229-238.

CAIRNS, S. H., DICKSON, K. L. & ATKINSON, S. F. 1997. An Examination of Measuring Selected Water Quality Trophic Indicators with SPOT Satellite HRV Data. *Photogrammetric Engineering & Remote Sensing,* 63**,** 263-265.

CARTER, M. R. & GREGORICH, E. G. (eds.) 2008. *Soil sampling and methods of analysis*: CRC Press.

CHEN, C., TANG, S., PAN, Z., ZHAN, H., LARSON, M. & JÖNSSON, L. 2007a. Remotely sensed assessment of water quality levels in the Pearl River Estuary, China. *Marine Pollution Bulletin,* 54**,** 1267-1272.

CHEN, L. 2003. A study of applying genetic programming to reservoir trophic state evaluation using remote sensor data. *International Journal of Remote Sensing,* 24**,** 2265-2275.

CHEN, S., FANG, L., ZHANG, L. & HUANG, W. 2009. Remote sensing of turbidity in seawater intrusion reaches of Pearl River Estuary – A case study in Modaomen water way, China. *Estuarine, Coastal and Shelf Science,* 82**,** 119-127.

CHEN, Z., CURRAN, P. J. & HANSOM, J. D. 1992. Derivative reflective spectroscopy to estimate suspended sediment concentration. *Remote Sensing of Environment,* 40**,** 67-77.

CHEN, Z., HU, C. & MULLER-KARGER, F. 2007b. Monitoring turbidity in Tampa Bay using MODIS/Aqua 250-m imagery. *Remote Sensing of Environment,* 109**,** 207-220.

CLARK, B. J. F. 2010. *Enhanced processing of SPOT multispectral satellite imagery for environmental monitoring and modelling.* PhD, University of Helsinki.

CSIR 2010. A CSIR perspective on water in South Africa- 2010.

DAY, J. 2000. Biomonitoring: appropriate technology for the 21st century. *1st WARFSA/WaterNet Symposium: Sustainable Use of Water Resources.* Maputo.

DAY, J. A., DAVIES, B. R. & KING, J. M. 1986. Riverine Ecosystems.

DE LA REY, P. A., TAYLOR, J. C., LAAS, A., VAN RENSBURG, L. & VOSLOO, A. 2004. Determining the possible application value of diatoms as indicators of general water quality: A comparison with SASS 5. *Water SA,* 30**,** 325-332.

DEKKER, A. G., ZAMUROVIC-NENAD, Z., HOOGENBOOM, H. J. & PETERS, S. W. M. 1996. Remote sensing, ecological water quality modelling and in situ measurements: a case study in shallow lakes. *Hjâmtogkal Sciences Journal,* 41**,** 531-547.

DEMATTÊ, J. A. M., FIORIO, P. R. & ARAÚJO, S. R. 2010. Variation of routine soil analysis when compared with hyperspectral narrow band sensing method. *Remote Sensing,* 2**,** 1998-2016.

DOGLIOTTI, A. I., RUDDICK, K., NECHAD, B., LASTA, C., MERCADO, A., HOZBOR, C., GUERRERO, R., LÓPEZ, G. R. & ABELANDO, M. Calibration and validation of an algorithm for remote sensing of turbidity over La Plata river estuary, Argentina. EARSeL eProceedings, 2011.

DÖRGELOH, W. G. 1995. Fish distribution in relation to turbidity gradients in a man-made lake, Sterkfontein Dam (South Africa). *Water SA,* 21**,** 95-99.

DÖRGELOH, W. G., SEAMAN, M. T. & GAIGHER, I. G. 1993. The Physical and Chemical Limnology of Sterkfontein Dam, Eastern Orange Free State, South Africa. *Water SA,* 19**,** 177-184.

DORON, M., BÉLANGER, S., DOXARAN, D. & BABIN, M. 2011. Spectral variations in the near-infrared ocean reflectance. *Remote Sensing of Environment,* 115**,** 1617-1631.

DOXARAN, D., FROIDEFOND, J.-M., LAVENDER, S. & CASTAING, P. 2002. Spectral signature of highly turbid waters: Application with SPOT data to quantify suspended particulate matter concentrations. *Remote Sensing of Environment,* 81**,** 149-161.

DOXORAN, D., FROIDEFOND, J.-M. & CASTAING, P. 2002. A reflectance band ratio used to estimate suspended matter concentrations in sediment-dominated coastal waters. *International Journal of Remote Sensing,* 23**,** 5079-5085.

DU PLESSIS, J. 2006. *The Assessment of the Water Quality of the Hex River Catchment - North West Province.* MSc, University of Johannesburg.

DUAN, H., ZHANG, Y., ZHANG, B., SONG, K. & WANG, Z. 2007. Assessment of Chlorophyll-<i>a</i> Concentration and Trophic State for Lake Chagan Using Landsat TM and Field Spectral Data. *Environmental Monitoring and Assessment,* 129**,** 295-308.

EARLE, A., GOLDIN, J. & KGOMOTSO, P. 2005. Domestic Water Provision in the Democratic South Africa – changes and challenges. University of Pretoria.

EKERCIN, S. 2007. Water Quality Retrievals from High Resolution Ikonos Multispectral Imagery: A Case Study in Istanbul, Turkey. *Water Air Soil Pollution,* 183**,** 239-251.

EL-MASRI, B. & RAHMAN, A. F. Undated. Estimation of Water Quality Parameters for Lake Kemp Texas Derived From Remotely Sensed Data.

EVA, H. D., BRINK, A. B. & SIMONETTI, D. 2006. Monitoring land cover dynamics in sub-Saharan Africa. Luxembourg: Office for Official Publication of the European Communities.

FATOKI, O. S., MUYIMA, N. Y. O. & LUJIZA, N. 2001. Situation analysis of water quality in the Umtata River catchment. *Water SA,* 27**,** 467-473.

GIARDINO, C., BRANDO, V. E., DEKKER, A. G., STRÖMBECK, N. & CANDIANI, G. 2007. Assessment of water quality in Lake Garda (Italy) using Hyperion. *Remote Sensing of Environment,* 109**,** 183-195.

GONS, H. J. 1999. Optical teledetection of chlorophyll-a in turbid inland waters *Environmental Science and Technology,* 33**,** 1127-1132.

GOVENDER, M., CHETTY, K. & BULCOCK, H. 2007. A review of hyperspectral remote sensing and its application in vegetation and water resource studies. *Water SA* 33**,** 145-152.

GOVENDER, M., CHETTY, K. & BULCOCK, H. 2008. A comparison of satellite hyperspectral and multispectral remote sensing imagery for improved classification and mapping of vegetation. *Water SA,* 34**,** 147-154.

HABOUDANE, D., MILLER, J. R., PATTEY, E., ZARCO-TEJADA, P. J. & STRACHAN, I. B. 2004. Hyperspectral vegetation indices and novel algorithms for predicting green LAI of crop canopies: Modeling and validation in the context of precision agriculture. *Remote Sensing of Environment,* 90**,** 337-352.

HAN, L. & RUNDQUIST, D. C. 1997. Comparison of NIR/RED ratio and first derivative of reflectance in estimating algal-chlorophyll concentration: A case study in a turbid reservoir. *Remote Sensing of Environment,* 62**,** 253-261.

HAN, L. & RUNDQUIST, D. C. 1998. The impact of a wind-roughened water surface on remote measurements of turbidity. *International Journal of Remote Sensing,* 19**,** 195-201.

HART, R. C. 1999. On the limnology of Spioenkop, a turbid reservoir on the upper Thukela River, with particular reference to the structure and dynamics of its plankton community. *Water SA* 25**,** 519-528.

HE, W., CHEN, S., LIU, X. & CHEN, J. 2008. Water quality monitoring in slightly-polluted inland water body through remote sensing- A case study in Guanting Reservoir, Beijing, China. *Frontiers of Environmental Science & Engineering in China,* 2**,** 163-171.

HELLWEGER, F. L., MILLER, W. & OSHODI, K. S. 2007. Mapping Turbidity in the Charles River, Boston Using a High-resolution Satellite. *Environment Monitoring and Assessment,* 132**,** 311-320.

HELLWEGER, F. L., SCHLOSSER, P., LALL, U. & WEISSEL, J. K. 2004. Use of satellite imagery for water quality studies in New York Harbor. *Estuarine, Coastal and Shelf Science,* 61**,** 437-448.

HONGVE, D. & ÅKESSON, G. 1998. Comparison of Nephelometric Turbidity Measurements Using Wavelengths 400-600 and 860 nm. *Water Resources,* 32**,** 3143-3145.

HUANG, Y., JIANG, D., DAFANG, Z. & FU, J. 2010. Evaluation of Hyperspectral Indices for Chlorophyll-a Concentration Estimation in Tangxun Lake (Wuhan, China). *International Journal of Environmental Research and Public Health,* 7**,** 2437-2451.

JENSEN, J. R. 2000. *Remote Sensing of the Environment: An Earth resources perspectives,* Upper Saddle River, N. Y., Prentice Hall, Inc.

KARABULUT, M. & CEYLAN, N. 2005. The Spectral Reflectance Responses of Water with Different Levels

of Suspended Sediment in The Presence of Algae. *Turkish Journal of Engineering and Environmental Science,* 29**,** 351-360.

KAUTH, R. J. & THOMAS, G. S. The tasseled cap - a graphic description of the spectral-temporal development of agricultural crops as seen by Landsat. Proceedings of the Symposium on Machine Processing of Remotely Sensed Data, 29 June-1 July 1976 Purdue University, West Lafayette, Indiana (West Lafayette, Indiana: Laboratory for Applications of Remote Sensing). 41-51.

KHORRAM, S., CHESHIRE, H., GERACI, A. L. & ROSA, G. L. 1991. Water quality mapping of Augusta Bay, Italy from Landsat-TM data. *International Journal of Remote Sensing,* 12**,** 803-808.

KOPONEN, S. 2006. *Remote sensing of water quality for Finnish lakes and coastal areas.* PhD, Helsinki University of Technology.

KOPONEN, S., PULLIAINEN, J., KALLIO, K. & HALLIKAINEN, M. 2002. Lake water quality classification with airborne hyperspectral spectrometer and simulated MERIS data. *Remote Sensing of Environment,* 79**,** 51-59.

KRIJGSMAN, J. 1994. *Optical remote sensing of water quality parameters: Interpretation of reflectance spectra.* PhD Dissertation, Delft University of Technology.

KUTSER, T., PIERSON, D. C., KALLIO, K. Y., REINART, A. & SOBEK, S. 2005. Mapping lake CDOM by satellite remote sensing. *Remote Sensing of Environment* 94**,** 535–540.

KWOH, K. L., NG, S. M., KUAN, H. N., CHIA, K., LIEW, S. C., CHANG, C. W. & KWOH, L. K. Undated. Investigating relationship of nephelometric turbidity unit and total suspended solids with the inherent optical properties parameters derived from spectra reflectance.

LAMBROU, T. P., ANASTASIOU, C. C. & PANAYIOTOU, C. G. 2010. A Nephelometric Turbidity System for Monitoring Residential Drinking Water Quality. *In:* KOMNINOS, N. (ed.) *Sensor Applications, Experimentation, and Logistics.* Athens, Greece: Springer Berlin Heidelberg.

LATHROP, R. G., JR & LILLESAND, T. M. 1986. Use of Thematic Mapper data to assess water quality in Green Bay and central Lake Michigan. *Photogrammetric Engineering and Remote Sensing,* 52**,** 671-680.

LILLESAND, T. M., KIEFER, R. W. & CHIPMAN, J. W. 2004. *Remote Sensing and Image Interpretation (5th Ed.),* New York, John Wiley and Sons, Inc.

LIU, B., ZHANG, L., ZHANG, X., ZHANG, B. & TONG, Q. 2009. Simulation of EO-1 Hyperion Data from ALI Multispectral Data Based on the Spectral Reconstruction Approach. *Sensors,* 9 3090-3108

LIU, Y., ISLAM, M. A. & GAO, J. 2003. Quantification of shallow water quality parameters by means of remote sensing. *Progress in Physical Geography,* 27**,** 24-43.

LODHI, M. A., RUNDQUIST, D. C., HAN, L. & KUZILA, M. S. 1997. The potential for remote sensing of loess soils suspended in surface waters. *Journal of the American Water Resources Association,* 33**,** 111-117.

MATTHEWS, M. W., BERNARD, S. & WINTER, K. 2010. Remote sensing of cyanobacteria-dominant algal blooms and water quality parameters in Zeekoevlei, a small hypertrophic lake, using MERIS. *Remote Sensing of Environment,* 114**,** 2070-2087.

MILLER, R. L. & MCKEE, B. A. 2004. Using MODIS Terra 250 m imagery to map concentrations of total suspended matter in coastal waters. *Remote Sensing of Environment,* 93**,** 259-266.

MINELLA, J. P. G., MERTEN, G. H., REICHERT, J. M. & CLARKE, R. T. 2008. Estimating suspended sediment concentrations from turbidity measurements and the calibration problem. *Hydrological Processes,* 22**,** 1819-1830.

MOORE, G. K. 1980. Satellite remote sensing of water turbidity. *Hydrological Science-Bulletin,* 25**,** 407-421.

MOREL, A. & PRIEUR, L. 1977. Analysis of variations in ocean color. *Limnology and Oceanography,* 22**,** 709-722.

MORENO-MADRINAN, M. J., AL-HAMDAN, M. Z., RICKMAN, D. L. & MULLER-KARGER, F. E. 2010. Using the Surface Reflectance MODIS Terra Product to Estimate Turbidity in Tampa Bay, Florida. *Remote Sensing,* 2**,** 2713-2728.

MUTANGA, O. & RUGEGE, D. 2006. Integrating remote sensing and spatial statistics to model herbaceous biomass distribution in a tropical savanna. *International Journal of Remote Sensing,* 27**,** 3499-3514.

NGWENYA, F. 2006. *Water Quality Trends in the Eerste River, Western Cape, 1990-2005.* MSc Minithesis, University of the Western Cape.

NORSALIZA, U. & HASMADI, I. M. 2010a. Analysis of SPOT- 5 Data for Mapping Turbidity Level of River Klang Peninsular Malaysia. *Applied Remote Sensing Journal,* 1**,** 14-18.

NORSALIZA, U. & HASMADI, M. I. 2010b. Use of Remote Sensing and GIS in Monitoring Water Quality. *Journal of Sustainable Development,* 3**,** 228-238.

NOVO, E. M. L. M., FILHO, W. P. & MELACK, J. M. 2004. Assessing the utility of spectral band operators to reduce the influence of total suspended solids on the relationship between chlorophyll concentration and the bidirectional reflectance factor in Amazon waters. *International Journal of Remote Sensing,* 25**,** 5105-5116.

NWRS 2004. National Water Resource Strategy. First ed. Pretoria: Department of Water Affairs and Forestry (DWAF).

OLET, E. 2010. *Water Quality Monitoring of Roxo reservoir using Landsat Images and In-situ Measurements.* MSc, International Institute of Geo-Information Science and Earth Observation (ITC).

OMAR, A. F. & MATJAFRI, M. Z. 2009. Turbidimeter Design and Analysis: A Review on Optical Fiber Sensors for the Measurement of Water Turbidity. *Sensors,* 9**,** 8311-8335.

ÖSTLUND, C., FLINK, P., STRÖMBECK, N., PIERSON, D. & LINDELL, T. 2001. Mapping of the water quality of Lake Erken, Sweden, from Imaging Spectrometry and Landsat Thematic Mapper. *Science of the Total Environment,* 268**,** 139-154.

OUILLON, S., DOUILLET, P., PETRENKO, A., NEVEUX, J., DUPOUY, C., FROIDEFOND, J.-M., ANDRÉFOUËT, S. & MUÑOZ-CARAVACA, A. 2008. Optical Algorithms at Satellite Wavelengths for Total Suspended Matter in Tropical Coastal Waters. *Sensors,* 8**,** 4165-4185.

PAVELSKY, T. M. & SMITH, L. C. 2009. Remote sensing of suspended sediment concentration, flow velocity, and lake recharge in the Peace-Athabasca Delta, Canada. *Water Resources Research,* 45.

PENG, F., EFFLERA, S. W., PIERSON, D. C. & SMITH, D. G. 2009. Light-scattering features of turbidity-causing particles in interconnected reservoir basins and a connecting stream. *Water Research,* 43**,** 2280-2292.

PETUS, C., CHUST, G., GOHIN, F., DOXARAN, D., FROIDEFOND, J.-M. & SAGARMINAGA, Y. 2010. Estimating turbidity and total suspended matter in the

Adour River plume (South Bay of Biscay) using MODIS 250-m imagery. *Continental Shelf Research,* 30**,** 379-392.

PLAZA, J., MARTINEZ, P. J., PEREZ, R. M., PLAZA, A. & CANTERO, C. 2004. Nonlinear neural-network-based mixture model for estimating the concentration of nitrogen salts in turbid inland waters using hyperspectral imagery. Chemical and Biological Standoff Detection II, Wednesday 27 October 2004 Philadelphia, PA, USA.

POTES, M., COSTA, M. J. & SALGADO, R. 2012. Satellite remote sensing of water turbidity in Alqueva reservoir and implications on lake modelling. *Hydrology and Earth System Sciences,* 16**,** 1623-1633.

RAMOLLO, P. P. 2008. *Bioassessing the Impact of Water Quality on the Health And Parasite Composition of Oreochromis Mossambicus at the Phalaborwa Industrial Complex (Pic) and the Barrage (Olifants River) in the Limpopo Province, South Africa.* MSc, University of Limpopo.

RAZMKHAH, H., ABRISHAMCHI, A. & TORKIAN, A. 2010. Evaluation of spatial and temporal variation in water quality by pattern recognition techniques: A case study on Jajrood River (Tehran, Iran). *Journal of Environmental Management,* 91**,** 852-860.

RIZZO, L., BELGIORNO, V. & CASALE, R. 2005. Simultaneous compliance of TOC and turbidity related to pathogen breakthrough and THMs control by enhanced coagulation. *Global NEST Journal,* 7**,** 145-153.

ROSSEL, V. R. A., WALVOORT, D. J. J., MCBRATNEY, A. B., JANIK, L. J. & SKJEMSTAD, J. O. 2006. Visible, near infrared, mid infrared or combined diffuse reflectance spectroscopy for simultaneous assessment of various soil properties. *Geoderma,* 131**,** 59-75.

ROUSE, J. W., HAAS, R. H., DEERING, D. W. & SEHELL, J. A. 1974. Monitoring the vernal advancement and retrogradation (Green wave effect) of natural vegetation. Remote Sensing Center, Texas A&M Univ., College Station.

RUDDICK, K. G., DE CAUWER, V., PARK, Y.-J. & MOORE, G. 2006. Seaborne measurements of near infrared water-leaving reflectance: The similarity spectrum for turbid waters. *Limnology and Oceanography,* 51**,** 1167-1179.

SADAR, M. Turbidity instrumentation - an overview of today's available technology. Turbidity and Other Sediment Surrogates Workshop, April 30 – May 2 2002 Reno, NV.

SADAR, M. J. Undated. Turbidity Science: Technical Information Series- Booklet No. 11.

SADAR, M. J. & ENGELHARDT, T. L. Undated. Determining correlation of nephelometric turbidity measurements to suspended solids in industrial samples.

SANTINI, F., ALBEROTANZA, L., CAVALLI, R. M. & PIGNATTI, S. 2010. A two-step optimization procedure for assessing water constituent concentrations by hyperspectral remote sensing techniques: An application to the highly turbid Venice lagoon waters. *Remote Sensing of Environment,* 114**,** 887-898.

SCHULZE, R. E. 1995. Hydrology and Agrohydrology: A text to accompany the ACRU 3.00 Agrohydrological Modelling System. Pretoria, RSA: Water Research Commission.

SECOR, T. D. 2006. *Quantifying Chlorophyll A Content through Remote Sensing: A Pilot Study of Utah Lake.* Minithesis, Brigham Young University.

SENAY, G. B., SHAFIQUE, N. A., AUTREY, B. C., FULK, F. & CORMIER, S. M. 2001. The Selection of Narrow Wavebands for Optimizing Water Quality Monitoring on the Great Miami River, Ohio using Hyperspectral Remote Sensor Data. *Journal of Spatial Hydrology,* 1**,** 1-22.

SHAFIQUE, N. A., FULK, F., AUTREY, B. C. & FLOTEMERSCH, J. 2003. Hyperspectral Remote Sensing of Water Quality Parameters for Large Rivers in the Ohio River Basin. Available: http://www.tucson.ars.ag.gov/icrw/Proceedings/Shafique.pdf.

SHEELA, A. M., SABU, J., LETHA, J. & RAMACHANDRAN, K. K. 2010. Prediction of Water Quality of a Lake System by Relating Secchi Disk Depth and IRS P6 Radiance Data. *ICTT 2010*. College of Engineering, Trivandrum.

SHIBAYAMA, M., KANDA, K. & SUGAHARA, K. 2007. Water turbidity estimation using a hand-held spectropolarimeter to determine surface reflection polarization in visible, near and short-wave infrared bands. *International Journal of Remote Sensing,* 28**,** 3747-3755.

SHIKLOMANOV, I. A. 1998. World Water Resources: A new appraisal and assessment for the 21st Century. International Hydrological Programme report ed. Paris: UNESCO.

SINGH, R. 2010. Geotechnical investigation for the Msunduzi Waterfront Development, Pietermaritzburg. Terratest.Accessed from: www.terratest.co.za/files/downloads/Camps Drift/Appendix H - Geotech.pdf

STERCKX, S., KNAEPS, E., BOLLEN, M., TROUW, K. & HOUTHUYS, R. 2007. Retrieval of Suspended Sediment from Advanced Hyperspectral Sensor Data in the Scheldt Estuary at Different Stages in the Tidal Cycle. *Marine Geodesy,* 30, 1-12.

SU, H., SHENG, Y. & DU, P. 2008a. A New Band Selection Algorithm for Hyperspectral Data Based on Fractal Dimension. *The International Archives of the Photogrammetry, Remote Sensing and Spatial Information Sciences,* XXXVII**,** 279-284.

SU, Y.-F., LIOU, J.-J., HOU, J.-C., HUNG, W.-C., HSU, S.-M., LIEN, Y.-T., SU, M.-D., CHENG, K.-S. & WANG, Y.-F. 2008b. A Multivariate Model for Coastal Water Quality Mapping Using Satellite Remote Sensing Images. *Sensors,* 8**,** 6321-6339.

SUDHEER, K. P., CHAUBEY, I. & GARG, V. 2006. Lake Water Quality Assessment From Landsat Thematic Mapper Data Using Neural Network: An Approach to Optimal Band Combination Selection.N. *Journal of the American Water Resources Association,* 42**,** 1683-1695.

SUGIHARA, S., KISHINO, M. & OKAMI, N. 1985. Estimation of water quality parameters from irradiance reflectance using optical models. *Journal of Oceanography,* 41**,** 399-406.

THIEMANN, S. & KAUFMANN, H. 2000. Determination of Chlorophyll Content and Trophic State of Lakes Using Field Spectrometer and IRS-1C Satellite Data in the Mecklenburg Lake District, Germany. *Remote Sensing of Environment,* 73**,** 227-235.

TURDUKULOV, U. 2003. *Determination of water quality parameters using imaging spectrometry - A case study for the Sajo floodplain, Hungary.* MSc, International Institute for Geo-Information Science and Earth Observation.

TURDUKULOV, U. & VEKERDY, Z. 2003. Determination of water quality parameters using imaging spectrometry – case study for the Sajó floodplain, Hungary. *3rd EARSeL Workshop on Imaging Spectroscopy.* Herrsching, Germany.

VAN DER MERWE-BOTHA, M. 2009. Water quality: A vital dimension of water security. Midrand: DBSA.

VAN VLIET, H. R. & NELL, U. 1986. Surface Water Quality of South Africa. The Vaal River Catchment: 1979 to 1983. Pretoria: Hydrological Research Institute (DWAF Technical Report TR131).

VENTER, A. 2002. *Water quality in the Rustenburg Dorpspruit.* MSc Short Dissertation, Rand Afrikaanse University.

VOLPE, V., SILVESTRI, S. & MARANI, M. 2011. Remote sensing retrieval of suspended sediment concentration in shallow waters. *Remote Sensing of Environment,* 115**,** 44-54.

WANG, F., HAN, L., KUNG, H. T. & VAN ARSDALE, R. B. 2006. Applications of Landsat5 TM imageru in assessing and mapping water quality in Reelfoot Lake, Tennessee. *International Journal of Remote Sensing,* 27**,** 5269-5283.

WANG, J.-J., LU, X.-X., ZHOU, Y. & LIEW, S.-C. 2013. Suspended sediment concentrations estimate in highly turbid rivers: a field spectral survey. *Remote Sensing Letters,* 4, 4, 409-417.

WHITMORE, J. S. 1971 South Africa's water budget. *South African Journal of Science,* 67**,** 166-17.

WONG, M. S., NICHOL, J. E., LEE, K. H. & EMERSON, N. 2008. Modeling Water Quality Using Terra/Modis 500m Satellite Images. *The International Archives of the Photogrammetry, Remote Sensing and Spatial Information Sciences,* 37**,** 679-684.

WRC. 1998. Assessment guide. *In:* MANYAKA, M. S. & PIETERSEN, A. (eds.) *Quality of domestic water supplies.*

WU, G., DE LEEUW, J., SKIDMORE, A. K., PRINS, H. H. T. & LIU, Y. 2007. Concurrent monitoring of vessels and water turbidity enhances the strength of evidence in remotely sensed dredging impact assessment. *Water Research,* 41**,** 3271-3280.

YAMAGUCHI, Y. & NAITO, C. 2003. Spectral indices for lithologic discrimination and mapping by using the ASTER SWIR bands. *International Journal of Remote Sensing,* 24**,** 4311-4323.

YANG, M. D., SYKES, R. M. & MERRY, C. J. 2000. Estimation of algal biological parameters using water quality modeling and SPOT satellite data. *Ecological Modelling,* 125**,** 1-13.

YANG, X. & JIN, W. 2010. GIS-based spatial regression and prediction of water quality in river networks: A case study in Iowa. *Journal of Environmental Management,* 91**,** 1943-1951.

ZHENGJUN, W., JIANMING, H. & GUISEN, D. 2008. Use of satellite imagery to assess the trophic state of Miyun Reservoir, Beijing, China. *Environmental Pollution,* 155**,** 13-19.

ZIEGLER, A. C. Issues related to use of turbidity measurements as a surrogate for suspended sediment. Turbidity and Other Sediment Surrogates Workshop, Turbidity and Other Sediment Surrogates Workshop 2002 Reno, NV.

APPENDIX A: SPECTRAL DATA

Sample	Clear water	X10	X20	X30	X40	X50	X60	X70	X80	X90	X100	X110	X120	X130	X140	X150
400	0.0353	0.0228	0.0412	0.0389	0.0613	0.0645	0.0809	0.0624	0.0895	0.0627	0.0745	0.0688	0.0795	0.0834	0.0888	0.0663
401	0.0392	0.0232	0.0435	0.0417	0.0638	0.0677	0.0845	0.0652	0.0945	0.0656	0.0788	0.0713	0.0827	0.0870	0.0930	0.0699
402	0.0392	0.0250	0.0447	0.0428	0.0663	0.0702	0.0881	0.0677	0.0970	0.0684	0.0806	0.0749	0.0863	0.0906	0.0966	0.0720
403	0.0392	0.0257	0.0459	0.0442	0.0684	0.0727	0.0902	0.0695	0.1002	0.0702	0.0841	0.0774	0.0891	0.0945	0.1002	0.0752
404	0.0392	0.0267	0.0471	0.0456	0.0706	0.0749	0.0927	0.0717	0.1030	0.0724	0.0870	0.0795	0.0920	0.0970	0.1037	0.0766
405	0.0431	0.0267	0.0490	0.0471	0.0717	0.0766	0.0952	0.0738	0.1055	0.0738	0.0888	0.0816	0.0938	0.0995	0.1055	0.0795
406	0.0431	0.0271	0.0498	0.0474	0.0731	0.0781	0.0959	0.0756	0.1084	0.0756	0.0906	0.0834	0.0955	0.1020	0.1084	0.0809
407	0.0431	0.0285	0.0502	0.0481	0.0745	0.0795	0.0980	0.0759	0.1094	0.0770	0.0920	0.0856	0.0980	0.1037	0.1102	0.0827
408	0.0431	0.0289	0.0506	0.0499	0.0763	0.0809	0.0998	0.0788	0.1112	0.0784	0.0941	0.0870	0.0995	0.1062	0.1123	0.0845
409	0.0431	0.0296	0.0529	0.0510	0.0777	0.0824	0.1020	0.0795	0.1137	0.0795	0.0963	0.0891	0.1016	0.1073	0.1148	0.0859
410	0.0431	0.0307	0.0533	0.0513	0.0781	0.0841	0.1037	0.0806	0.1152	0.0813	0.0977	0.0909	0.1037	0.1112	0.1169	0.0873
411	0.0431	0.0310	0.0541	0.0528	0.0813	0.0856	0.1052	0.0827	0.1187	0.0831	0.1002	0.0930	0.1066	0.1130	0.1194	0.0898
412	0.0471	0.0321	0.0561	0.0545	0.0824	0.0884	0.1080	0.0841	0.1209	0.0848	0.1023	0.0948	0.1091	0.1148	0.1226	0.0920
413	0.0471	0.0328	0.0569	0.0553	0.0848	0.0895	0.1098	0.0873	0.1241	0.0873	0.1052	0.0966	0.1112	0.1184	0.1248	0.0945
414	0.0471	0.0335	0.0588	0.0567	0.0863	0.0920	0.1119	0.0888	0.1258	0.0891	0.1062	0.1002	0.1144	0.1205	0.1291	0.0963
415	0.0471	0.0346	0.0596	0.0588	0.0877	0.0941	0.1144	0.0909	0.1287	0.0906	0.1102	0.1016	0.1159	0.1241	0.1305	0.0995
416	0.0471	0.0353	0.0604	0.0595	0.0902	0.0963	0.1176	0.0923	0.1312	0.0923	0.1127	0.1041	0.1191	0.1266	0.1340	0.1009
417	0.0510	0.0364	0.0624	0.0606	0.0916	0.0984	0.1191	0.0948	0.1340	0.0948	0.1148	0.1070	0.1219	0.1287	0.1365	0.1034
418	0.0510	0.0374	0.0631	0.0620	0.0938	0.1002	0.1216	0.0970	0.1362	0.0959	0.1173	0.1087	0.1234	0.1316	0.1394	0.1052
419	0.0510	0.0378	0.0643	0.0635	0.0952	0.1016	0.1241	0.0988	0.1387	0.0984	0.1198	0.1116	0.1262	0.1348	0.1419	0.1080
420	0.0510	0.0389	0.0659	0.0645	0.0970	0.1041	0.1262	0.1002	0.1405	0.1002	0.1219	0.1134	0.1294	0.1365	0.1447	0.1102
421	0.0510	0.0396	0.0667	0.0656	0.0988	0.1055	0.1280	0.1023	0.1433	0.1016	0.1234	0.1152	0.1305	0.1405	0.1476	0.1127
422	0.0510	0.0403	0.0690	0.0670	0.1002	0.1073	0.1301	0.1041	0.1455	0.1037	0.1266	0.1176	0.1330	0.1412	0.1497	0.1144
423	0.0510	0.0414	0.0698	0.0684	0.1012	0.1091	0.1319	0.1048	0.1476	0.1052	0.1280	0.1191	0.1351	0.1440	0.1522	0.1155
424	0.0510	0.0421	0.0698	0.0684	0.1030	0.1102	0.1333	0.1080	0.1490	0.1062	0.1298	0.1212	0.1373	0.1462	0.1540	0.1173
425	0.0510	0.0424	0.0706	0.0699	0.1045	0.1127	0.1355	0.1080	0.1526	0.1087	0.1312	0.1226	0.1387	0.1479	0.1569	0.1198
426	0.0510	0.0439	0.0737	0.0717	0.1059	0.1141	0.1376	0.1116	0.1540	0.1105	0.1344	0.1251	0.1412	0.1504	0.1597	0.1219
427	0.0549	0.0446	0.0737	0.0727	0.1084	0.1166	0.1405	0.1123	0.1572	0.1116	0.1362	0.1269	0.1447	0.1544	0.1622	0.1244
428	0.0549	0.0456	0.0761	0.0749	0.1116	0.1194	0.1437	0.1155	0.1608	0.1152	0.1398	0.1305	0.1472	0.1576	0.1658	0.1280
429	0.0549	0.0478	0.0776	0.0777	0.1137	0.1219	0.1483	0.1191	0.1643	0.1184	0.1433	0.1344	0.1515	0.1615	0.1704	0.1312
430	0.0549	0.0488	0.0816	0.0806	0.1176	0.1266	0.1522	0.1226	0.1697	0.1219	0.1479	0.1380	0.1565	0.1668	0.1761	0.1351
431	0.0588	0.0513	0.0835	0.0831	0.1219	0.1319	0.1572	0.1269	0.1761	0.1262	0.1529	0.1430	0.1622	0.1725	0.1829	0.1405
432	0.0588	0.0531	0.0875	0.0863	0.1269	0.1373	0.1636	0.1319	0.1832	0.1316	0.1590	0.1494	0.1683	0.1790	0.1900	0.1462
433	0.0627	0.0563	0.0914	0.0906	0.1316	0.1422	0.1708	0.1380	0.1897	0.1365	0.1654	0.1558	0.1758	0.1872	0.1975	0.1519
434	0.0627	0.0585	0.0961	0.0941	0.1376	0.1487	0.1779	0.1430	0.1982	0.1437	0.1725	0.1619	0.1825	0.1947	0.2053	0.1597
435	0.0667	0.0610	0.0996	0.0988	0.1437	0.1551	0.1854	0.1494	0.2068	0.1497	0.1811	0.1690	0.1907	0.2029	0.2150	0.1658
436	0.0667	0.0645	0.1031	0.1027	0.1490	0.1619	0.1925	0.1561	0.2157	0.1554	0.1886	0.1758	0.1989	0.2121	0.2239	0.1743
437	0.0706	0.0667	0.1075	0.1073	0.1561	0.1683	0.1996	0.1633	0.2235	0.1615	0.1957	0.1836	0.2071	0.2207	0.2332	0.1797
438	0.0706	0.0692	0.1125	0.1112	0.1615	0.1747	0.2068	0.1686	0.2317	0.1683	0.2032	0.1904	0.2146	0.2292	0.2410	0.1872
439	0.0745	0.0713	0.1165	0.1155	0.1661	0.1804	0.2139	0.1754	0.2392	0.1740	0.2107	0.1968	0.2214	0.2367	0.2499	0.1936
440	0.0745	0.0745	0.1204	0.1191	0.1733	0.1857	0.2207	0.1804	0.2467	0.1793	0.2168	0.2036	0.2285	0.2456	0.2578	0.2007
441	0.0784	0.0777	0.1239	0.1230	0.1772	0.1918	0.2282	0.1868	0.2556	0.1854	0.2246	0.2111	0.2371	0.2528	0.2663	0.2068
442	0.0784	0.0806	0.1286	0.1276	0.1836	0.1986	0.2353	0.1932	0.2624	0.1918	0.2314	0.2189	0.2442	0.2610	0.2759	0.2135
443	0.0824	0.0831	0.1329	0.1316	0.1904	0.2053	0.2428	0.1993	0.2713	0.1975	0.2392	0.2250	0.2524	0.2699	0.2841	0.2210
444	0.0824	0.0856	0.1369	0.1362	0.1954	0.2118	0.2506	0.2061	0.2795	0.2039	0.2463	0.2328	0.2595	0.2781	0.2934	0.2282

445	0.0863	0.0884	0.1408	0.1405	0.2004	0.2178	0.2567	0.2121	0.2877	0.2096	0.2542	0.2396	0.2677	0.2863	0.3016	0.2346
446	0.0863	0.0909	0.1443	0.1440	0.2068	0.2232	0.2635	0.2178	0.2955	0.2146	0.2606	0.2460	0.2749	0.2941	0.3098	0.2414
447	0.0863	0.0934	0.1475	0.1469	0.2114	0.2285	0.2692	0.2235	0.3016	0.2207	0.2670	0.2520	0.2816	0.3009	0.3176	0.2471
448	0.0902	0.0952	0.1510	0.1501	0.2150	0.2332	0.2745	0.2278	0.3077	0.2250	0.2734	0.2567	0.2877	0.3073	0.3241	0.2524
449	0.0902	0.0966	0.1537	0.1533	0.2193	0.2374	0.2791	0.2324	0.3130	0.2292	0.2781	0.2627	0.2934	0.3137	0.3298	0.2567
450	0.0902	0.0991	0.1565	0.1554	0.2221	0.2410	0.2831	0.2364	0.3180	0.2328	0.2827	0.2674	0.2977	0.3180	0.3358	0.2606
451	0.0902	0.0998	0.1588	0.1576	0.2253	0.2439	0.2859	0.2385	0.3216	0.2353	0.2870	0.2709	0.3020	0.3223	0.3401	0.2649
452	0.0941	0.1020	0.1604	0.1594	0.2278	0.2471	0.2895	0.2417	0.3251	0.2385	0.2898	0.2738	0.3055	0.3262	0.3437	0.2674
453	0.0941	0.1027	0.1608	0.1615	0.2292	0.2481	0.2913	0.2428	0.3276	0.2403	0.2923	0.2759	0.3077	0.3291	0.3469	0.2706
454	0.0941	0.1034	0.1635	0.1626	0.2307	0.2503	0.2927	0.2453	0.3298	0.2421	0.2945	0.2781	0.3102	0.3316	0.3487	0.2724
455	0.0941	0.1041	0.1639	0.1633	0.2324	0.2513	0.2941	0.2463	0.3308	0.2435	0.2966	0.2802	0.3119	0.3340	0.3519	0.2742
456	0.0941	0.1045	0.1643	0.1651	0.2335	0.2531	0.2966	0.2485	0.3333	0.2453	0.2980	0.2820	0.3144	0.3358	0.3537	0.2766
457	0.0941	0.1059	0.1647	0.1658	0.2346	0.2549	0.2977	0.2499	0.3348	0.2463	0.3009	0.2838	0.3159	0.3390	0.3561	0.2781
458	0.0941	0.1066	0.1671	0.1661	0.2367	0.2556	0.2991	0.2517	0.3369	0.2488	0.3016	0.2863	0.3184	0.3408	0.3576	0.2802
459	0.0941	0.1066	0.1678	0.1672	0.2374	0.2567	0.3005	0.2524	0.3387	0.2492	0.3034	0.2870	0.3198	0.3422	0.3594	0.2806
460	0.0902	0.1073	0.1682	0.1676	0.2374	0.2574	0.3005	0.2535	0.3390	0.2499	0.3045	0.2877	0.3205	0.3430	0.3611	0.2813
461	0.0902	0.1073	0.1682	0.1676	0.2378	0.2570	0.3005	0.2535	0.3390	0.2496	0.3045	0.2881	0.3205	0.3430	0.3611	0.2824
462	0.0902	0.1073	0.1678	0.1676	0.2378	0.2567	0.2998	0.2531	0.3387	0.2492	0.3045	0.2884	0.3201	0.3430	0.3611	0.2820
463	0.0902	0.1066	0.1678	0.1676	0.2364	0.2563	0.2980	0.2524	0.3365	0.2492	0.3037	0.2881	0.3201	0.3426	0.3601	0.2809
464	0.0902	0.1066	0.1651	0.1668	0.2349	0.2549	0.2966	0.2517	0.3355	0.2478	0.3020	0.2870	0.3191	0.3412	0.3590	0.2806
465	0.0902	0.1062	0.1651	0.1658	0.2346	0.2531	0.2952	0.2503	0.3333	0.2471	0.3009	0.2852	0.3176	0.3394	0.3558	0.2795
466	0.0863	0.1059	0.1647	0.1651	0.2328	0.2521	0.2934	0.2488	0.3319	0.2456	0.2991	0.2845	0.3159	0.3376	0.3551	0.2781
467	0.0863	0.1048	0.1631	0.1640	0.2314	0.2513	0.2920	0.2478	0.3301	0.2439	0.2984	0.2838	0.3152	0.3369	0.3537	0.2766
468	0.0863	0.1045	0.1627	0.1640	0.2310	0.2506	0.2913	0.2471	0.3287	0.2439	0.2970	0.2824	0.3137	0.3351	0.3529	0.2759
469	0.0863	0.1045	0.1627	0.1640	0.2310	0.2503	0.2906	0.2471	0.3280	0.2439	0.2966	0.2816	0.3134	0.3348	0.3522	0.2759
470	0.0863	0.1048	0.1631	0.1640	0.2310	0.2506	0.2906	0.2471	0.3280	0.2442	0.2966	0.2820	0.3134	0.3355	0.3522	0.2759
471	0.0863	0.1052	0.1631	0.1647	0.2310	0.2510	0.2906	0.2474	0.3283	0.2442	0.2966	0.2831	0.3141	0.3362	0.3522	0.2766
472	0.0824	0.1055	0.1631	0.1654	0.2310	0.2513	0.2909	0.2478	0.3283	0.2446	0.2977	0.2841	0.3144	0.3365	0.3529	0.2774
473	0.0824	0.1059	0.1639	0.1658	0.2321	0.2517	0.2913	0.2485	0.3291	0.2449	0.2984	0.2848	0.3152	0.3376	0.3537	0.2781
474	0.0824	0.1066	0.1647	0.1665	0.2321	0.2524	0.2923	0.2492	0.3298	0.2456	0.2984	0.2852	0.3162	0.3380	0.3547	0.2784
475	0.0824	0.1066	0.1651	0.1668	0.2328	0.2524	0.2930	0.2503	0.3308	0.2460	0.2998	0.2859	0.3166	0.3387	0.3551	0.2791
476	0.0824	0.1073	0.1651	0.1668	0.2335	0.2528	0.2934	0.2503	0.3308	0.2467	0.3002	0.2866	0.3176	0.3398	0.3558	0.2799
477	0.0824	0.1077	0.1651	0.1672	0.2339	0.2531	0.2930	0.2506	0.3316	0.2471	0.3002	0.2870	0.3176	0.3401	0.3561	0.2809
478	0.0824	0.1077	0.1663	0.1672	0.2339	0.2531	0.2930	0.2513	0.3316	0.2478	0.3002	0.2873	0.3176	0.3401	0.3561	0.2809
479	0.0824	0.1073	0.1659	0.1672	0.2332	0.2528	0.2920	0.2513	0.3301	0.2471	0.3002	0.2866	0.3169	0.3394	0.3558	0.2809
480	0.0784	0.1070	0.1643	0.1668	0.2324	0.2520	0.2902	0.2499	0.3291	0.2463	0.2998	0.2859	0.3162	0.3380	0.3544	0.2795
481	0.0784	0.1066	0.1631	0.1658	0.2296	0.2492	0.2877	0.2478	0.3258	0.2435	0.2970	0.2834	0.3134	0.3351	0.3515	0.2766
482	0.0784	0.1052	0.1616	0.1629	0.2267	0.2456	0.2834	0.2446	0.3212	0.2406	0.2930	0.2802	0.3098	0.3312	0.3472	0.2734
483	0.0745	0.1034	0.1580	0.1608	0.2228	0.2417	0.2791	0.2403	0.3152	0.2364	0.2881	0.2756	0.3045	0.3258	0.3412	0.2692
484	0.0745	0.1020	0.1561	0.1583	0.2196	0.2381	0.2738	0.2371	0.3098	0.2332	0.2834	0.2713	0.2995	0.3209	0.3358	0.2652
485	0.0745	0.1009	0.1545	0.1565	0.2164	0.2357	0.2706	0.2342	0.3062	0.2303	0.2791	0.2681	0.2955	0.3159	0.3312	0.2617
486	0.0706	0.1005	0.1529	0.1558	0.2153	0.2335	0.2684	0.2317	0.3027	0.2282	0.2770	0.2652	0.2934	0.3141	0.3276	0.2592
487	0.0706	0.1005	0.1529	0.1558	0.2153	0.2335	0.2684	0.2317	0.3023	0.2278	0.2763	0.2649	0.2920	0.3127	0.3266	0.2592
488	0.0706	0.1012	0.1549	0.1565	0.2164	0.2353	0.2699	0.2332	0.3034	0.2292	0.2766	0.2652	0.2938	0.3141	0.3280	0.2602
489	0.0706	0.1027	0.1565	0.1590	0.2182	0.2371	0.2717	0.2353	0.3066	0.2310	0.2791	0.2684	0.2963	0.3162	0.3308	0.2620
490	0.0706	0.1037	0.1584	0.1608	0.2203	0.2399	0.2749	0.2381	0.3098	0.2339	0.2824	0.2713	0.2991	0.3198	0.3348	0.2652
491	0.0706	0.1052	0.1600	0.1622	0.2232	0.2424	0.2774	0.2399	0.3119	0.2364	0.2845	0.2734	0.3016	0.3226	0.3376	0.2677

492	0.0706	0.1066	0.1608	0.1640	0.2239	0.2439	0.2784	0.2424	0.3141	0.2374	0.2873	0.2759	0.3030	0.3248	0.3394	0.2699
493	0.0706	0.1070	0.1620	0.1647	0.2253	0.2449	0.2795	0.2435	0.3152	0.2396	0.2884	0.2774	0.3052	0.3258	0.3408	0.2702
494	0.0706	0.1073	0.1624	0.1654	0.2260	0.2463	0.2806	0.2453	0.3166	0.2399	0.2891	0.2781	0.3066	0.3266	0.3419	0.2713
495	0.0706	0.1080	0.1643	0.1661	0.2278	0.2471	0.2820	0.2463	0.3176	0.2406	0.2906	0.2795	0.3070	0.3280	0.3426	0.2724
496	0.0706	0.1080	0.1643	0.1672	0.2282	0.2474	0.2820	0.2471	0.3176	0.2410	0.2913	0.2795	0.3070	0.3283	0.3437	0.2738
497	0.0706	0.1080	0.1651	0.1672	0.2282	0.2467	0.2813	0.2471	0.3173	0.2410	0.2906	0.2791	0.3070	0.3280	0.3430	0.2731
498	0.0667	0.1080	0.1647	0.1668	0.2264	0.2463	0.2791	0.2463	0.3155	0.2399	0.2895	0.2784	0.3055	0.3262	0.3412	0.2720
499	0.0667	0.1080	0.1635	0.1665	0.2260	0.2460	0.2784	0.2456	0.3152	0.2399	0.2884	0.2784	0.3048	0.3255	0.3405	0.2713
500	0.0667	0.1084	0.1639	0.1665	0.2260	0.2460	0.2784	0.2460	0.3148	0.2396	0.2888	0.2781	0.3048	0.3248	0.3398	0.2706
501	0.0667	0.1102	0.1647	0.1679	0.2271	0.2467	0.2791	0.2471	0.3155	0.2406	0.2895	0.2784	0.3048	0.3255	0.3408	0.2717
502	0.0667	0.1112	0.1659	0.1686	0.2289	0.2496	0.2824	0.2485	0.3173	0.2421	0.2898	0.2799	0.3070	0.3280	0.3426	0.2738
503	0.0667	0.1119	0.1686	0.1704	0.2310	0.2513	0.2848	0.2517	0.3198	0.2453	0.2930	0.2827	0.3091	0.3298	0.3455	0.2759
504	0.0667	0.1130	0.1694	0.1725	0.2342	0.2545	0.2873	0.2542	0.3237	0.2478	0.2966	0.2863	0.3130	0.3333	0.3494	0.2791
505	0.0667	0.1159	0.1725	0.1758	0.2371	0.2578	0.2906	0.2574	0.3273	0.2506	0.2998	0.2898	0.3169	0.3369	0.3533	0.2827
506	0.0667	0.1169	0.1749	0.1768	0.2396	0.2602	0.2938	0.2606	0.3308	0.2538	0.3030	0.2916	0.3194	0.3401	0.3565	0.2852
507	0.0667	0.1184	0.1765	0.1797	0.2421	0.2635	0.2973	0.2645	0.3340	0.2556	0.3059	0.2948	0.3226	0.3437	0.3604	0.2884
508	0.0667	0.1198	0.1784	0.1811	0.2446	0.2660	0.2984	0.2667	0.3355	0.2578	0.3080	0.2980	0.3255	0.3465	0.3626	0.2906
509	0.0667	0.1212	0.1804	0.1836	0.2456	0.2674	0.3009	0.2684	0.3387	0.2599	0.3102	0.2995	0.3280	0.3494	0.3651	0.2930
510	0.0667	0.1223	0.1816	0.1843	0.2478	0.2699	0.3023	0.2706	0.3405	0.2617	0.3130	0.3023	0.3294	0.3508	0.3676	0.2945
511	0.0667	0.1237	0.1835	0.1854	0.2492	0.2709	0.3037	0.2717	0.3419	0.2627	0.3134	0.3030	0.3301	0.3522	0.3683	0.2952
512	0.0667	0.1241	0.1839	0.1865	0.2492	0.2713	0.3037	0.2724	0.3422	0.2635	0.3141	0.3034	0.3312	0.3526	0.3690	0.2959
513	0.0667	0.1244	0.1835	0.1861	0.2488	0.2709	0.3023	0.2724	0.3408	0.2624	0.3137	0.3030	0.3301	0.3519	0.3683	0.2952
514	0.0667	0.1234	0.1827	0.1854	0.2478	0.2699	0.3005	0.2709	0.3387	0.2617	0.3123	0.3020	0.3283	0.3497	0.3651	0.2934
515	0.0667	0.1234	0.1820	0.1854	0.2471	0.2684	0.3002	0.2706	0.3369	0.2613	0.3105	0.2991	0.3266	0.3480	0.3636	0.2916
516	0.0627	0.1241	0.1831	0.1861	0.2474	0.2695	0.3005	0.2709	0.3373	0.2613	0.3102	0.2995	0.3266	0.3480	0.3633	0.2923
517	0.0627	0.1255	0.1859	0.1889	0.2499	0.2727	0.3041	0.2738	0.3401	0.2631	0.3127	0.3023	0.3291	0.3501	0.3661	0.2952
518	0.0667	0.1280	0.1898	0.1925	0.2549	0.2784	0.3098	0.2788	0.3465	0.2688	0.3173	0.3070	0.3348	0.3554	0.3722	0.2998
519	0.0667	0.1319	0.1945	0.1979	0.2617	0.2863	0.3184	0.2852	0.3554	0.2756	0.3241	0.3144	0.3422	0.3643	0.3804	0.3073
520	0.0667	0.1358	0.2016	0.2046	0.2692	0.2945	0.3266	0.2941	0.3651	0.2834	0.3330	0.3234	0.3522	0.3736	0.3914	0.3159
521	0.0667	0.1405	0.2067	0.2100	0.2766	0.3023	0.3348	0.3030	0.3743	0.2916	0.3430	0.3316	0.3608	0.3843	0.4018	0.3244
522	0.0706	0.1440	0.2114	0.2139	0.2827	0.3087	0.3415	0.3098	0.3825	0.2970	0.3508	0.3398	0.3686	0.3918	0.4096	0.3316
523	0.0706	0.1469	0.2149	0.2182	0.2877	0.3137	0.3465	0.3155	0.3882	0.3020	0.3569	0.3451	0.3750	0.3979	0.4160	0.3365
524	0.0706	0.1490	0.2188	0.2217	0.2916	0.3176	0.3504	0.3194	0.3932	0.3059	0.3611	0.3490	0.3793	0.4029	0.4207	0.3405
525	0.0706	0.1519	0.2220	0.2242	0.2955	0.3216	0.3554	0.3241	0.3971	0.3094	0.3654	0.3533	0.3840	0.4075	0.4257	0.3447
526	0.0706	0.1533	0.2267	0.2282	0.2995	0.3273	0.3608	0.3287	0.4039	0.3144	0.3704	0.3583	0.3889	0.4128	0.4314	0.3494
527	0.0706	0.1569	0.2306	0.2335	0.3059	0.3333	0.3679	0.3358	0.4114	0.3212	0.3768	0.3654	0.3954	0.4200	0.4396	0.3554
528	0.0745	0.1615	0.2373	0.2389	0.3137	0.3415	0.3768	0.3440	0.4207	0.3283	0.3847	0.3725	0.4043	0.4292	0.4478	0.3629
529	0.0745	0.1658	0.2427	0.2456	0.3212	0.3501	0.3857	0.3522	0.4307	0.3365	0.3936	0.3818	0.4132	0.4392	0.4588	0.3722
530	0.0745	0.1697	0.2490	0.2503	0.3276	0.3576	0.3929	0.3594	0.4381	0.3440	0.4018	0.3889	0.4225	0.4471	0.4677	0.3786
531	0.0745	0.1729	0.2529	0.2549	0.3323	0.3622	0.3979	0.3658	0.4446	0.3487	0.4082	0.3957	0.4271	0.4535	0.4745	0.3843
532	0.0745	0.1761	0.2565	0.2578	0.3369	0.3672	0.4025	0.3708	0.4496	0.3529	0.4128	0.4004	0.4324	0.4578	0.4791	0.3889
533	0.0745	0.1779	0.2604	0.2620	0.3412	0.3725	0.4082	0.3761	0.4553	0.3576	0.4175	0.4050	0.4374	0.4635	0.4848	0.3936
534	0.0784	0.1811	0.2643	0.2663	0.3462	0.3779	0.4139	0.3815	0.4613	0.3626	0.4228	0.4096	0.4435	0.4688	0.4913	0.3996
535	0.0784	0.1847	0.2694	0.2709	0.3515	0.3843	0.4196	0.3875	0.4677	0.3679	0.4296	0.4164	0.4496	0.4752	0.4973	0.4053
536	0.0784	0.1882	0.2733	0.2749	0.3558	0.3886	0.4246	0.3925	0.4738	0.3725	0.4346	0.4214	0.4545	0.4809	0.5041	0.4096
537	0.0784	0.1893	0.2765	0.2777	0.3594	0.3925	0.4275	0.3971	0.4777	0.3765	0.4389	0.4246	0.4578	0.4845	0.5073	0.4132
538	0.0784	0.1918	0.2780	0.2791	0.3626	0.3950	0.4303	0.3996	0.4799	0.3786	0.4410	0.4267	0.4602	0.4873	0.5098	0.4153

539	0.0784	0.1932	0.2812	0.2820	0.3651	0.3982	0.4335	0.4032	0.4831	0.3811	0.4431	0.4296	0.4631	0.4898	0.5130	0.4171
540	0.0784	0.1961	0.2843	0.2859	0.3690	0.4029	0.4381	0.4075	0.4881	0.3857	0.4474	0.4339	0.4674	0.4948	0.5176	0.4214
541	0.0784	0.1996	0.2890	0.2909	0.3747	0.4089	0.4449	0.4143	0.4952	0.3914	0.4531	0.4399	0.4724	0.4998	0.5244	0.4278
542	0.0784	0.2036	0.2953	0.2963	0.3822	0.4171	0.4531	0.4217	0.5037	0.3986	0.4610	0.4463	0.4809	0.5084	0.5323	0.4346
543	0.0784	0.2082	0.3024	0.3030	0.3897	0.4250	0.4613	0.4310	0.5130	0.4064	0.4692	0.4545	0.4895	0.5173	0.5415	0.4417
544	0.0784	0.2125	0.3067	0.3084	0.3964	0.4324	0.4684	0.4385	0.5216	0.4128	0.4770	0.4624	0.4980	0.5248	0.5494	0.4492
545	0.0784	0.2164	0.3125	0.3130	0.4018	0.4385	0.4756	0.4456	0.5291	0.4196	0.4834	0.4688	0.5045	0.5316	0.5576	0.4556
546	0.0824	0.2193	0.3176	0.3187	0.4075	0.4453	0.4806	0.4510	0.5351	0.4242	0.4891	0.4745	0.5098	0.5376	0.5636	0.4610
547	0.0824	0.2228	0.3224	0.3230	0.4139	0.4510	0.4870	0.4585	0.5419	0.4307	0.4959	0.4809	0.5166	0.5447	0.5697	0.4667
548	0.0824	0.2278	0.3286	0.3287	0.4196	0.4588	0.4945	0.4645	0.5490	0.4371	0.5023	0.4870	0.5230	0.5515	0.5775	0.4727
549	0.0824	0.2321	0.3349	0.3355	0.4271	0.4660	0.5020	0.4731	0.5576	0.4439	0.5091	0.4941	0.5312	0.5590	0.5861	0.4795
550	0.0824	0.2364	0.3416	0.3415	0.4342	0.4749	0.5112	0.4813	0.5676	0.4520	0.5176	0.5020	0.5390	0.5683	0.5947	0.4870
551	0.0824	0.2414	0.3478	0.3476	0.4417	0.4827	0.5187	0.4898	0.5754	0.4585	0.5251	0.5098	0.5469	0.5758	0.6032	0.4948
552	0.0824	0.2460	0.3537	0.3537	0.4485	0.4906	0.5262	0.4980	0.5847	0.4649	0.5330	0.5169	0.5544	0.5836	0.6107	0.5016
553	0.0824	0.2496	0.3608	0.3597	0.4553	0.4977	0.5340	0.5055	0.5918	0.4724	0.5408	0.5237	0.5619	0.5911	0.6189	0.5087
554	0.0863	0.2535	0.3647	0.3640	0.4613	0.5037	0.5394	0.5127	0.5989	0.4781	0.5469	0.5305	0.5672	0.5968	0.6257	0.5137
555	0.0824	0.2567	0.3686	0.3679	0.4656	0.5084	0.5440	0.5176	0.6036	0.4824	0.5519	0.5344	0.5711	0.6014	0.6299	0.5176
556	0.0824	0.2585	0.3722	0.3704	0.4677	0.5116	0.5462	0.5205	0.6061	0.4845	0.5544	0.5369	0.5743	0.6036	0.6332	0.5205
557	0.0824	0.2599	0.3745	0.3729	0.4706	0.5134	0.5487	0.5234	0.6082	0.4873	0.5561	0.5380	0.5758	0.6053	0.6342	0.5216
558	0.0824	0.2631	0.3780	0.3765	0.4738	0.5180	0.5529	0.5273	0.6121	0.4913	0.5586	0.5419	0.5786	0.6082	0.6374	0.5248
559	0.0824	0.2667	0.3831	0.3811	0.4799	0.5248	0.5594	0.5340	0.6185	0.4955	0.5643	0.5465	0.5847	0.6139	0.6428	0.5298
560	0.0824	0.2706	0.3902	0.3882	0.4873	0.5323	0.5672	0.5419	0.6267	0.5027	0.5704	0.5533	0.5914	0.6207	0.6510	0.5365
561	0.0824	0.2756	0.3957	0.3929	0.4941	0.5405	0.5754	0.5494	0.6353	0.5102	0.5772	0.5604	0.5989	0.6285	0.6588	0.5437
562	0.0824	0.2795	0.4016	0.3982	0.4991	0.5465	0.5811	0.5561	0.6421	0.5155	0.5840	0.5672	0.6050	0.6335	0.6656	0.5490
563	0.0824	0.2816	0.4055	0.4021	0.5045	0.5508	0.5854	0.5622	0.6474	0.5198	0.5889	0.5711	0.6096	0.6392	0.6702	0.5533
564	0.0824	0.2841	0.4094	0.4050	0.5084	0.5547	0.5889	0.5665	0.6510	0.5237	0.5929	0.5740	0.6121	0.6414	0.6738	0.5561
565	0.0824	0.2856	0.4114	0.4082	0.5109	0.5583	0.5918	0.5701	0.6535	0.5262	0.5943	0.5775	0.6157	0.6442	0.6770	0.5583
566	0.0824	0.2891	0.4133	0.4100	0.5134	0.5622	0.5947	0.5733	0.6574	0.5298	0.5979	0.5807	0.6189	0.6471	0.6799	0.5611
567	0.0824	0.2891	0.4169	0.4128	0.5169	0.5651	0.5975	0.5772	0.6613	0.5319	0.6004	0.5832	0.6200	0.6488	0.6820	0.5633
568	0.0824	0.2920	0.4180	0.4143	0.5194	0.5672	0.5986	0.5800	0.6631	0.5337	0.6032	0.5847	0.6232	0.6503	0.6845	0.5654
569	0.0824	0.2927	0.4200	0.4157	0.5205	0.5697	0.6007	0.5818	0.6652	0.5351	0.6036	0.5857	0.6235	0.6510	0.6852	0.5658
570	0.0824	0.2948	0.4235	0.4185	0.5241	0.5725	0.6039	0.5857	0.6681	0.5383	0.6061	0.5886	0.6253	0.6531	0.6884	0.5683
571	0.0824	0.2977	0.4278	0.4228	0.5291	0.5775	0.6082	0.5904	0.6724	0.5426	0.6093	0.5922	0.6292	0.6574	0.6923	0.5715
572	0.0824	0.3005	0.4322	0.4271	0.5337	0.5836	0.6139	0.5961	0.6784	0.5469	0.6153	0.5971	0.6349	0.6620	0.6973	0.5768
573	0.0824	0.3030	0.4353	0.4299	0.5365	0.5868	0.6160	0.6007	0.6824	0.5508	0.6189	0.6011	0.6374	0.6649	0.7002	0.5790
574	0.0824	0.3030	0.4357	0.4303	0.5376	0.5868	0.6150	0.6011	0.6824	0.5508	0.6196	0.6011	0.6371	0.6649	0.7002	0.5790
575	0.0784	0.3030	0.4357	0.4299	0.5355	0.5850	0.6135	0.6004	0.6802	0.5494	0.6171	0.5996	0.6357	0.6624	0.6980	0.5768
576	0.0784	0.3034	0.4357	0.4299	0.5351	0.5847	0.6125	0.6004	0.6788	0.5483	0.6160	0.5975	0.6342	0.6606	0.6955	0.5768
577	0.0784	0.3034	0.4361	0.4303	0.5351	0.5847	0.6125	0.6004	0.6781	0.5480	0.6157	0.5968	0.6335	0.6588	0.6952	0.5758
578	0.0784	0.3052	0.4369	0.4314	0.5358	0.5865	0.6139	0.6004	0.6784	0.5490	0.6157	0.5982	0.6335	0.6595	0.6955	0.5765
579	0.0784	0.3062	0.4404	0.4346	0.5394	0.5897	0.6164	0.6043	0.6816	0.5522	0.6189	0.6000	0.6357	0.6624	0.6970	0.5775
580	0.0784	0.3091	0.4443	0.4385	0.5433	0.5939	0.6207	0.6086	0.6856	0.5561	0.6225	0.6043	0.6403	0.6670	0.7023	0.5822
581	0.0784	0.3119	0.4475	0.4421	0.5476	0.5982	0.6250	0.6135	0.6909	0.5608	0.6275	0.6093	0.6456	0.6720	0.7066	0.5865
582	0.0784	0.3127	0.4506	0.4442	0.5504	0.6011	0.6282	0.6175	0.6941	0.5643	0.6307	0.6128	0.6488	0.6752	0.7102	0.5900
583	0.0784	0.3130	0.4506	0.4449	0.5508	0.6011	0.6278	0.6182	0.6941	0.5640	0.6317	0.6128	0.6488	0.6745	0.7102	0.5900
584	0.0745	0.3119	0.4482	0.4424	0.5480	0.5982	0.6235	0.6153	0.6916	0.5611	0.6296	0.6114	0.6460	0.6720	0.7073	0.5879
585	0.0745	0.3087	0.4447	0.4381	0.5437	0.5922	0.6175	0.6114	0.6856	0.5569	0.6253	0.6064	0.6410	0.6660	0.7020	0.5818

586	0.0745	0.3045	0.4376	0.4303	0.5358	0.5843	0.6089	0.6043	0.6777	0.5497	0.6182	0.5993	0.6328	0.6574	0.6941	0.5758
587	0.0706	0.2973	0.4259	0.4189	0.5255	0.5704	0.5947	0.5936	0.6645	0.5398	0.6071	0.5889	0.6203	0.6435	0.6820	0.5654
588	0.0667	0.2884	0.4149	0.4075	0.5134	0.5579	0.5804	0.5800	0.6503	0.5280	0.5936	0.5761	0.6068	0.6289	0.6681	0.5526
589	0.0667	0.2841	0.4094	0.4018	0.5066	0.5522	0.5733	0.5733	0.6424	0.5219	0.5847	0.5676	0.5975	0.6193	0.6581	0.5455
590	0.0667	0.2873	0.4125	0.4057	0.5102	0.5565	0.5790	0.5758	0.6460	0.5255	0.5847	0.5690	0.5993	0.6210	0.6610	0.5490
591	0.0667	0.2913	0.4184	0.4111	0.5166	0.5636	0.5868	0.5832	0.6531	0.5308	0.5914	0.5758	0.6061	0.6282	0.6670	0.5551
592	0.0667	0.2934	0.4220	0.4150	0.5201	0.5676	0.5907	0.5875	0.6578	0.5348	0.5968	0.5800	0.6111	0.6324	0.6724	0.5594
593	0.0667	0.2941	0.4235	0.4160	0.5212	0.5679	0.5904	0.5886	0.6578	0.5351	0.5971	0.5811	0.6114	0.6332	0.6724	0.5597
594	0.0667	0.2948	0.4239	0.4175	0.5216	0.5686	0.5914	0.5897	0.6574	0.5355	0.5971	0.5818	0.6118	0.6328	0.6724	0.5601
595	0.0667	0.2966	0.4271	0.4196	0.5241	0.5715	0.5925	0.5914	0.6592	0.5376	0.5993	0.5832	0.6139	0.6357	0.6738	0.5615
596	0.0667	0.2980	0.4302	0.4228	0.5262	0.5743	0.5954	0.5936	0.6617	0.5398	0.6007	0.5847	0.6157	0.6367	0.6752	0.5626
597	0.0667	0.3002	0.4314	0.4264	0.5283	0.5761	0.5982	0.5950	0.6624	0.5412	0.6032	0.5868	0.6178	0.6399	0.6763	0.5643
598	0.0667	0.3009	0.4345	0.4275	0.5291	0.5768	0.5989	0.5971	0.6627	0.5412	0.6043	0.5872	0.6182	0.6399	0.6766	0.5636
599	0.0627	0.3012	0.4353	0.4292	0.5298	0.5772	0.5986	0.5971	0.6624	0.5415	0.6032	0.5875	0.6178	0.6399	0.6759	0.5633
600	0.0627	0.3020	0.4357	0.4303	0.5298	0.5775	0.5989	0.5979	0.6617	0.5415	0.6025	0.5868	0.6168	0.6396	0.6745	0.5633
601	0.0627	0.3027	0.4369	0.4317	0.5301	0.5793	0.6000	0.5979	0.6617	0.5430	0.6025	0.5868	0.6178	0.6396	0.6745	0.5633
602	0.0627	0.3048	0.4400	0.4342	0.5340	0.5829	0.6039	0.6011	0.6649	0.5447	0.6050	0.5893	0.6200	0.6428	0.6766	0.5651
603	0.0627	0.3073	0.4435	0.4381	0.5380	0.5868	0.6086	0.6043	0.6692	0.5487	0.6086	0.5936	0.6239	0.6463	0.6802	0.5693
604	0.0627	0.3084	0.4459	0.4410	0.5394	0.5893	0.6096	0.6078	0.6720	0.5512	0.6121	0.5968	0.6267	0.6492	0.6834	0.5715
605	0.0627	0.3084	0.4459	0.4410	0.5390	0.5886	0.6089	0.6075	0.6713	0.5508	0.6111	0.5968	0.6267	0.6485	0.6831	0.5715
606	0.0627	0.3077	0.4443	0.4396	0.5383	0.5872	0.6068	0.6061	0.6688	0.5494	0.6100	0.5950	0.6246	0.6467	0.6816	0.5697
607	0.0627	0.3070	0.4435	0.4381	0.5362	0.5857	0.6057	0.6046	0.6663	0.5476	0.6071	0.5936	0.6232	0.6456	0.6788	0.5679
608	0.0627	0.3059	0.4424	0.4378	0.5351	0.5840	0.6036	0.6025	0.6638	0.5465	0.6064	0.5914	0.6221	0.6424	0.6770	0.5668
609	0.0588	0.3059	0.4424	0.4374	0.5351	0.5832	0.6025	0.6021	0.6635	0.5458	0.6050	0.5904	0.6203	0.6424	0.6749	0.5661
610	0.0588	0.3059	0.4424	0.4381	0.5351	0.5843	0.6032	0.6021	0.6635	0.5462	0.6050	0.5904	0.6210	0.6424	0.6756	0.5661
611	0.0588	0.3062	0.4435	0.4396	0.5355	0.5850	0.6032	0.6025	0.6635	0.5465	0.6057	0.5914	0.6214	0.6424	0.6763	0.5661
612	0.0588	0.3055	0.4424	0.4392	0.5351	0.5836	0.6018	0.6025	0.6624	0.5462	0.6043	0.5914	0.6203	0.6421	0.6749	0.5654
613	0.0588	0.3045	0.4424	0.4378	0.5330	0.5825	0.6011	0.6018	0.6602	0.5444	0.6036	0.5900	0.6189	0.6399	0.6731	0.5647
614	0.0588	0.3041	0.4408	0.4367	0.5319	0.5815	0.5986	0.5996	0.6581	0.5430	0.6014	0.5882	0.6168	0.6385	0.6717	0.5622
615	0.0588	0.3037	0.4400	0.4360	0.5305	0.5790	0.5968	0.5982	0.6560	0.5426	0.5996	0.5868	0.6160	0.6360	0.6699	0.5615
616	0.0588	0.3037	0.4408	0.4374	0.5308	0.5818	0.5982	0.5982	0.6563	0.5426	0.5993	0.5868	0.6150	0.6360	0.6692	0.5611
617	0.0588	0.3055	0.4447	0.4414	0.5355	0.5861	0.6032	0.6021	0.6617	0.5472	0.6029	0.5911	0.6200	0.6403	0.6742	0.5654
618	0.0588	0.3087	0.4502	0.4467	0.5408	0.5922	0.6093	0.6089	0.6688	0.5526	0.6082	0.5971	0.6264	0.6471	0.6806	0.5715
619	0.0588	0.3109	0.4514	0.4481	0.5433	0.5947	0.6118	0.6128	0.6717	0.5554	0.6125	0.6011	0.6303	0.6510	0.6845	0.5743
620	0.0588	0.3105	0.4510	0.4481	0.5437	0.5939	0.6111	0.6135	0.6706	0.5554	0.6139	0.6025	0.6303	0.6510	0.6845	0.5750
621	0.0588	0.3087	0.4490	0.4456	0.5408	0.5907	0.6064	0.6111	0.6670	0.5519	0.6114	0.5993	0.6275	0.6471	0.6820	0.5715
622	0.0549	0.3062	0.4447	0.4421	0.5365	0.5854	0.6014	0.6061	0.6610	0.5476	0.6064	0.5947	0.6217	0.6424	0.6756	0.5672
623	0.0549	0.3034	0.4416	0.4385	0.5319	0.5807	0.5968	0.6011	0.6556	0.5437	0.6007	0.5897	0.6171	0.6367	0.6695	0.5629
624	0.0549	0.3012	0.4384	0.4357	0.5283	0.5779	0.5925	0.5968	0.6510	0.5401	0.5954	0.5850	0.6121	0.6324	0.6652	0.5590
625	0.0549	0.2998	0.4369	0.4342	0.5266	0.5754	0.5904	0.5954	0.6481	0.5383	0.5936	0.5825	0.6096	0.6296	0.6620	0.5561
626	0.0549	0.2991	0.4357	0.4321	0.5262	0.5750	0.5889	0.5943	0.6478	0.5365	0.5914	0.5822	0.6075	0.6267	0.6606	0.5547
627	0.0549	0.2970	0.4325	0.4299	0.5226	0.5715	0.5850	0.5914	0.6428	0.5337	0.5882	0.5779	0.6039	0.6221	0.6563	0.5508
628	0.0510	0.2955	0.4302	0.4271	0.5201	0.5679	0.5815	0.5879	0.6396	0.5308	0.5847	0.5750	0.6004	0.6178	0.6524	0.5480
629	0.0510	0.2941	0.4290	0.4267	0.5180	0.5665	0.5800	0.5847	0.6360	0.5291	0.5818	0.5722	0.5979	0.6157	0.6499	0.5455
630	0.0510	0.2930	0.4278	0.4260	0.5166	0.5647	0.5783	0.5836	0.6349	0.5276	0.5797	0.5704	0.5961	0.6143	0.6485	0.5447
631	0.0510	0.2927	0.4278	0.4260	0.5162	0.5647	0.5783	0.5832	0.6332	0.5276	0.5800	0.5708	0.5957	0.6143	0.6478	0.5444
632	0.0510	0.2927	0.4278	0.4267	0.5169	0.5651	0.5783	0.5836	0.6335	0.5276	0.5804	0.5715	0.5975	0.6150	0.6481	0.5458

633	0.0510	0.2934	0.4290	0.4267	0.5173	0.5654	0.5786	0.5840	0.6346	0.5283	0.5811	0.5725	0.5982	0.6164	0.6485	0.5465
634	0.0510	0.2923	0.4290	0.4267	0.5166	0.5654	0.5779	0.5840	0.6328	0.5283	0.5804	0.5722	0.5975	0.6153	0.6481	0.5458
635	0.0510	0.2923	0.4278	0.4264	0.5152	0.5651	0.5779	0.5832	0.6321	0.5280	0.5797	0.5711	0.5968	0.6153	0.6467	0.5455
636	0.0510	0.2923	0.4282	0.4271	0.5162	0.5654	0.5779	0.5836	0.6321	0.5287	0.5800	0.5718	0.5968	0.6153	0.6467	0.5455
637	0.0510	0.2923	0.4290	0.4275	0.5166	0.5654	0.5779	0.5840	0.6328	0.5291	0.5811	0.5733	0.5979	0.6164	0.6478	0.5465
638	0.0471	0.2913	0.4267	0.4260	0.5141	0.5626	0.5740	0.5818	0.6296	0.5262	0.5790	0.5708	0.5961	0.6143	0.6449	0.5444
639	0.0471	0.2884	0.4227	0.4217	0.5084	0.5561	0.5679	0.5761	0.6232	0.5212	0.5740	0.5668	0.5907	0.6082	0.6396	0.5394
640	0.0471	0.2852	0.4192	0.4182	0.5041	0.5519	0.5633	0.5711	0.6182	0.5173	0.5683	0.5611	0.5847	0.6021	0.6335	0.5344
641	0.0471	0.2852	0.4184	0.4178	0.5037	0.5515	0.5629	0.5697	0.6153	0.5162	0.5668	0.5594	0.5832	0.6004	0.6310	0.5330
642	0.0471	0.2848	0.4176	0.4178	0.5037	0.5512	0.5626	0.5701	0.6153	0.5162	0.5668	0.5597	0.5829	0.6004	0.6310	0.5333
643	0.0471	0.2838	0.4165	0.4160	0.5020	0.5490	0.5597	0.5686	0.6139	0.5148	0.5658	0.5590	0.5822	0.5986	0.6307	0.5323
644	0.0471	0.2816	0.4125	0.4121	0.4984	0.5447	0.5544	0.5654	0.6100	0.5116	0.5626	0.5558	0.5786	0.5950	0.6271	0.5294
645	0.0431	0.2770	0.4055	0.4050	0.4923	0.5373	0.5476	0.5594	0.6036	0.5066	0.5576	0.5515	0.5715	0.5886	0.6210	0.5241
646	0.0431	0.2717	0.3988	0.3971	0.4863	0.5308	0.5401	0.5544	0.5979	0.5012	0.5519	0.5451	0.5661	0.5815	0.6153	0.5187
647	0.0431	0.2677	0.3941	0.3925	0.4820	0.5251	0.5351	0.5490	0.5914	0.4966	0.5469	0.5405	0.5608	0.5761	0.6111	0.5144
648	0.0431	0.2667	0.3922	0.3911	0.4795	0.5230	0.5326	0.5451	0.5879	0.4941	0.5433	0.5369	0.5569	0.5722	0.6075	0.5109
649	0.0431	0.2677	0.3949	0.3939	0.4802	0.5244	0.5337	0.5447	0.5879	0.4945	0.5419	0.5362	0.5569	0.5725	0.6057	0.5105
650	0.0431	0.2695	0.3973	0.3968	0.4827	0.5280	0.5369	0.5483	0.5914	0.4970	0.5444	0.5390	0.5601	0.5754	0.6082	0.5141
651	0.0431	0.2709	0.3988	0.3989	0.4848	0.5301	0.5401	0.5522	0.5939	0.4995	0.5480	0.5422	0.5626	0.5783	0.6111	0.5169
652	0.0431	0.2709	0.3996	0.3989	0.4848	0.5301	0.5398	0.5522	0.5932	0.4995	0.5487	0.5426	0.5626	0.5779	0.6111	0.5166
653	0.0431	0.2688	0.3953	0.3950	0.4809	0.5237	0.5326	0.5476	0.5872	0.4945	0.5455	0.5390	0.5583	0.5736	0.6068	0.5116
654	0.0392	0.2599	0.3820	0.3825	0.4649	0.5066	0.5141	0.5319	0.5690	0.4791	0.5305	0.5244	0.5437	0.5572	0.5893	0.4959
655	0.0392	0.2481	0.3659	0.3647	0.4439	0.4841	0.4906	0.5077	0.5437	0.4585	0.5084	0.5023	0.5187	0.5326	0.5636	0.4745
656	0.0392	0.2471	0.3667	0.3679	0.4435	0.4863	0.4945	0.5030	0.5408	0.4556	0.4977	0.4938	0.5130	0.5266	0.5558	0.4709
657	0.0392	0.2570	0.3816	0.3832	0.4613	0.5062	0.5144	0.5201	0.5608	0.4734	0.5130	0.5098	0.5312	0.5462	0.5743	0.4873
658	0.0392	0.2688	0.3984	0.3996	0.4809	0.5266	0.5351	0.5426	0.5840	0.4941	0.5358	0.5330	0.5547	0.5690	0.5993	0.5080
659	0.0392	0.2731	0.4035	0.4061	0.4870	0.5333	0.5412	0.5519	0.5911	0.5002	0.5462	0.5422	0.5629	0.5790	0.6082	0.5155
660	0.0392	0.2749	0.4078	0.4107	0.4913	0.5387	0.5462	0.5569	0.5975	0.5048	0.5515	0.5480	0.5693	0.5843	0.6143	0.5201
661	0.0392	0.2770	0.4106	0.4118	0.4938	0.5405	0.5483	0.5601	0.5986	0.5070	0.5540	0.5504	0.5711	0.5875	0.6171	0.5226
662	0.0392	0.2774	0.4106	0.4118	0.4941	0.5401	0.5483	0.5604	0.5986	0.5070	0.5547	0.5515	0.5715	0.5879	0.6178	0.5230
663	0.0392	0.2766	0.4102	0.4114	0.4934	0.5398	0.5476	0.5597	0.5975	0.5066	0.5544	0.5497	0.5711	0.5868	0.6160	0.5226
664	0.0392	0.2777	0.4114	0.4139	0.4945	0.5412	0.5487	0.5604	0.5986	0.5080	0.5547	0.5519	0.5711	0.5875	0.6168	0.5226
665	0.0392	0.2777	0.4122	0.4146	0.4955	0.5426	0.5497	0.5626	0.6000	0.5098	0.5558	0.5537	0.5736	0.5900	0.6193	0.5244
666	0.0392	0.2777	0.4118	0.4146	0.4959	0.5426	0.5497	0.5626	0.6000	0.5094	0.5565	0.5537	0.5740	0.5900	0.6193	0.5244
667	0.0392	0.2781	0.4137	0.4157	0.4963	0.5433	0.5504	0.5633	0.6000	0.5098	0.5569	0.5544	0.5747	0.5907	0.6200	0.5255
668	0.0392	0.2784	0.4141	0.4168	0.4966	0.5447	0.5512	0.5647	0.6014	0.5109	0.5583	0.5558	0.5750	0.5911	0.6200	0.5258
669	0.0392	0.2784	0.4141	0.4168	0.4970	0.5444	0.5508	0.5647	0.6007	0.5109	0.5586	0.5558	0.5761	0.5914	0.6207	0.5258
670	0.0392	0.2774	0.4125	0.4150	0.4959	0.5426	0.5487	0.5633	0.5996	0.5098	0.5572	0.5551	0.5740	0.5893	0.6182	0.5244
671	0.0392	0.2770	0.4118	0.4160	0.4955	0.5426	0.5487	0.5619	0.5982	0.5094	0.5554	0.5533	0.5725	0.5882	0.6178	0.5234
672	0.0392	0.2774	0.4137	0.4171	0.4963	0.5440	0.5504	0.5643	0.6004	0.5102	0.5565	0.5551	0.5754	0.5897	0.6193	0.5251
673	0.0392	0.2781	0.4153	0.4182	0.4991	0.5465	0.5519	0.5658	0.6014	0.5130	0.5590	0.5572	0.5765	0.5918	0.6214	0.5273
674	0.0392	0.2784	0.4153	0.4189	0.4995	0.5469	0.5519	0.5668	0.6018	0.5134	0.5594	0.5579	0.5772	0.5922	0.6221	0.5276
675	0.0392	0.2795	0.4153	0.4200	0.4995	0.5480	0.5540	0.5683	0.6032	0.5141	0.5597	0.5594	0.5786	0.5936	0.6225	0.5283
676	0.0392	0.2799	0.4176	0.4210	0.5005	0.5487	0.5547	0.5690	0.6043	0.5155	0.5622	0.5604	0.5797	0.5954	0.6242	0.5301
677	0.0392	0.2799	0.4184	0.4221	0.5023	0.5497	0.5551	0.5708	0.6057	0.5176	0.5629	0.5622	0.5815	0.5961	0.6264	0.5312
678	0.0392	0.2802	0.4188	0.4228	0.5037	0.5519	0.5569	0.5722	0.6068	0.5176	0.5636	0.5633	0.5829	0.5975	0.6271	0.5326
679	0.0392	0.2802	0.4188	0.4235	0.5041	0.5522	0.5583	0.5736	0.6075	0.5187	0.5661	0.5647	0.5832	0.5986	0.6282	0.5340

680	0.0392	0.2802	0.4192	0.4250	0.5041	0.5529	0.5583	0.5736	0.6082	0.5201	0.5661	0.5658	0.5840	0.6000	0.6289	0.5340
681	0.0392	0.2802	0.4216	0.4253	0.5055	0.5540	0.5586	0.5758	0.6093	0.5209	0.5668	0.5665	0.5854	0.6004	0.6296	0.5344
682	0.0353	0.2802	0.4192	0.4250	0.5048	0.5526	0.5579	0.5754	0.6082	0.5209	0.5661	0.5665	0.5850	0.6004	0.6292	0.5344
683	0.0353	0.2795	0.4188	0.4225	0.5034	0.5508	0.5544	0.5733	0.6057	0.5187	0.5651	0.5654	0.5832	0.5975	0.6278	0.5333
684	0.0353	0.2759	0.4110	0.4157	0.4963	0.5415	0.5451	0.5676	0.5975	0.5119	0.5594	0.5579	0.5750	0.5904	0.6210	0.5248
685	0.0353	0.2645	0.3933	0.3964	0.4759	0.5180	0.5198	0.5469	0.5736	0.4898	0.5415	0.5398	0.5544	0.5665	0.5979	0.5045
686	0.0314	0.2474	0.3690	0.3708	0.4463	0.4863	0.4873	0.5112	0.5362	0.4570	0.5037	0.5023	0.5148	0.5248	0.5565	0.4692
687	0.0314	0.2389	0.3576	0.3608	0.4321	0.4731	0.4752	0.4906	0.5169	0.4410	0.4774	0.4788	0.4916	0.5005	0.5308	0.4492
688	0.0314	0.2456	0.3686	0.3725	0.4446	0.4891	0.4913	0.5023	0.5312	0.4531	0.4845	0.4873	0.5037	0.5127	0.5426	0.4606
689	0.0314	0.2521	0.3792	0.3832	0.4578	0.5023	0.5048	0.5187	0.5469	0.4688	0.5009	0.5045	0.5209	0.5301	0.5608	0.4763
690	0.0314	0.2578	0.3875	0.3914	0.4699	0.5148	0.5173	0.5337	0.5636	0.4827	0.5191	0.5212	0.5376	0.5483	0.5804	0.4920
691	0.0314	0.2606	0.3910	0.3954	0.4774	0.5212	0.5237	0.5444	0.5743	0.4923	0.5312	0.5337	0.5494	0.5608	0.5932	0.5034
692	0.0314	0.2585	0.3882	0.3911	0.4781	0.5209	0.5223	0.5494	0.5793	0.4963	0.5390	0.5398	0.5540	0.5654	0.6025	0.5098
693	0.0314	0.2563	0.3847	0.3875	0.4770	0.5198	0.5212	0.5494	0.5800	0.4966	0.5398	0.5415	0.5544	0.5654	0.6050	0.5112
694	0.0314	0.2585	0.3886	0.3918	0.4809	0.5251	0.5273	0.5533	0.5840	0.5009	0.5430	0.5451	0.5583	0.5693	0.6103	0.5159
695	0.0314	0.2645	0.3996	0.4036	0.4909	0.5373	0.5390	0.5622	0.5939	0.5102	0.5519	0.5544	0.5686	0.5793	0.6189	0.5241
696	0.0314	0.2724	0.4106	0.4150	0.5012	0.5483	0.5504	0.5747	0.6053	0.5209	0.5633	0.5658	0.5807	0.5936	0.6307	0.5344
697	0.0314	0.2724	0.4110	0.4160	0.5027	0.5497	0.5512	0.5786	0.6086	0.5230	0.5679	0.5701	0.5843	0.5971	0.6342	0.5373
698	0.0314	0.2688	0.4063	0.4096	0.4991	0.5447	0.5455	0.5750	0.6043	0.5201	0.5654	0.5668	0.5811	0.5932	0.6317	0.5344
699	0.0314	0.2652	0.4000	0.4039	0.4941	0.5390	0.5408	0.5704	0.6000	0.5159	0.5604	0.5629	0.5761	0.5868	0.6271	0.5301
700	0.0314	0.2645	0.3984	0.4021	0.4920	0.5373	0.5387	0.5686	0.5975	0.5144	0.5583	0.5597	0.5736	0.5847	0.6246	0.5287

APPENDIX B: SOIL ATTRIBUTES

	Soil samples										
	S1	S2	S3	S4	S5	S6	S7	S8	S9	S10	S11
Total % Nitrogen	0.13	0.16	0.15	0.33	0.27	0.22	0.22	0.23	0.24	0.22	0.24
Total % Carbon	1.91	2.06	2.04	3.6	3.2	2.67	2.62	2.68	2.67	2.44	2.65
Density (g/ml)	1.16	1.11	1.11	1.03	0.98	1.06	1.07	1.1	1.12	1.1	1.06
P (g/ml)	5	2	4	17	13	8	5	8	6	7	7
K (g/ml)	117	134	160	435	268	184	159	224	206	210	234
Ca (g/ml)	1851	1938	172	178	1784	1856	1952	1925	1915	1957	1968
Mg (g/ml)	665	730	757	813	731	678	705	694	757	749	756
Ex acidity (cmol/L)	0.05	0.05	0.04	0.08	0.13	0.08	0.1	0.08	0.11	0.08	0.06
Total cations (cmol/L)	15.05	16.06	7.54	8.77	15.73	15.39	16.05	15.97	16.42	16.55	16.7
Acid sat %	0	0	1	1	1	1	1	1	1	0	0
Ph (KCl)	5.06	5.09	5.12	4.99	4.98	5.09	5.11	5.37	4.98	5.1	5.14
Zn (g/ml)	4.4	4.7	5.2	9.3	7.7	9.1	7.2	7.5	6.1	7.5	7.9
Mn (g/ml)	120	120	44	100	220	120	120	120	130	180	170
Cu (g/ml)	6.7	6.5	7	7.8	7.5	7.3	7.8	6.5	6.9	7.3	6.6
Organic C %	1.7	1.6	1.8	2.6	2.9	2.1	2	1.9	2.2	1.9	1.9
N %	0.21	0.16	0.21	0.25	0.28	0.21	0.18	0.16	0.21	0.19	0.19
Clay %	38	40	44	42	43	40	38	39	40	39	42
Clay %	29	36	37	37	36	31	35	31	36	35	38
Fine Silt %	20	26	26	27	27	24	27	24	26	26	28
Coarse Silt & Sand %	51	39	38	36	37	45	38	46	39	39	34

APPENDIX C: PLOT OF R2 AND P VALUES FOR ALL BANDS